



Multi-scale temporal variability in biological-physical associations in the NE Chukchi Sea

Silvana Gonzalez¹ · John K. Horne¹ · Seth L. Danielson²

Received: 23 October 2020 / Revised: 2 March 2021 / Accepted: 4 March 2021
© The Author(s), under exclusive licence to Springer-Verlag GmbH Germany, part of Springer Nature 2021

Abstract

In high-latitude marine ecosystems, traditional net sampling is constrained to the ice-free season, resulting in an incomplete understanding of ecosystem structure and dynamics. Using 4 years of continuous acoustic and environmental measurements from a NE Chukchi Sea subsurface mooring, we assessed fish and zooplankton abundance and behavior relative to environmental factors over a wide range of temporal scales. We applied wavelet analysis to these high-resolution, multi-year, concurrent, and co-located datasets to identify temporal scales of variability in environmental conditions and density and vertical distribution metrics for pelagic fish and zooplankton. Biological variability occurs mainly at distinct diel (24-h), seasonal (3–6-month), and annual (9–12-month) scales. Diel patterns are present throughout the year but are strongest in autumn when day-night cycles are pronounced. Seasonal variability in zooplankton metrics (3–4 months) is mainly associated with sea ice patterns that may also regulate the onset of primary production. Seasonal variations in fish metrics are associated most closely with salinity patterns (~3 months) and slower changes in water temperature (~6 months). Annual cycles in biological characteristics are influenced by year-round variations in water temperature, sea ice concentration, light irradiance, and wind. Wind and salinity-associated variability in biological metrics was observed at scales of 6–28 days. Scale-dependent biological and environmental associations vary through time and emphasize the importance of high-resolution long-term studies for comprehensive ecosystem characterizations. Our results identify necessary scales of observation in Arctic monitoring programs for improved prediction and detection of biological responses to rapidly changing environments.

Keywords Acoustic backscatter · Polar cod · Chukchi Sea · Wavelets · Scale-dependency · Zooplankton

Introduction

Biological and physical processes that shape marine communities typically operate over multiple scales of space and time (Stommel 1963; Haury et al. 1978; Levin 1992; Schneider 1994). Consequently, efforts to attribute/associate observed variability with potential causes must also be conducted over a range of spatial and temporal scales (McIntire and Fajardo 2009). This approach increases our ability to detect, understand, and predict biological responses to environmental change (Horne and Schneider 1994), and identify relevant scales of variability for effective impact

assessments and resource management (Hewitt et al. 2007; Godø et al. 2014).

The dependence of observed patterns on observational scale coupled with potential trends over time increases the effort needed to understand temporal variability in biological variables. A complete characterization of time-dependent patterns requires high resolution and long-term (i.e. high scope) data. High scope data can be difficult to obtain due to available resources or constrained accessibility. These challenges are amplified in high latitude marine environments where the presence of sea ice during most of the year limits vessel-based sampling (e.g. Mueter et al. 2017; Spear et al. 2019). In these areas, data acquisition is typically limited in extent and/or resolution, fragmenting our understanding of important biological and physical processes occurring throughout the year. In particular, long term studies in the Pacific Arctic have focused on descriptions of biological variability from samples mainly collected during summer months either through systematic

✉ Silvana Gonzalez
silgonz@gmail.com

¹ School of Aquatic and Fishery Sciences, University of Washington, BOX 355020, Seattle, WA 98195, USA

² College of Fisheries and Ocean Sciences, University of Alaska Fairbanks, Fairbanks, AK 99775, USA

(e.g. Bluhm et al. 2010; Hopcroft and Day 2013; Moore and Stabeno 2015) or opportunistic (e.g. Ershova et al. 2015; Randall et al. 2019) surveys and data compilations. Studies examining high frequency temporal patterns (e.g. diel vertical migrations) over limited temporal extents (i.e. days to a few months) prevent an assessment of the consistency in observed patterns over longer periods (Fortier et al. 2001; Berge et al. 2009; Darnis et al. 2017; Geoffroy et al. 2017). A few studies have collected year-long biological data (e.g. Geoffroy et al. 2016; Kitamura et al. 2017) but the assessment of biological patterns over a continuum of temporal scales through multiple years remains uncommon.

The seasonally ice-covered Chukchi Sea receives a nearly continual input of heat, nutrients, organic carbon, and organisms from Pacific-origin water flowing northward in response to an oceanic pressure head that results from an elevation difference between the Pacific and Arctic Oceans (Stigebrandt 1984). This input from the Bering Sea, combined with shallow depths enhances biological productivity in the Chukchi Sea (Grebmeier et al. 2015). A large phytoplankton bloom that occurs in late spring and summer (Questel et al. 2013) supports the largest soft bottom benthic faunal biomass in the world ocean (Grebmeier et al. 2006, 2015), and corresponding populations of zooplankton (Ershova et al. 2015), seabirds (Kuletz et al. 2015), and marine mammals (Hannay et al. 2013). The Chukchi shelf is also home of polar cod (*Boreogadus saida*), a fish species that plays a key role in the transfer of energy from lower to higher trophic levels in high latitudes (Lowry and Frost 1981; Whitehouse et al. 2014). Located over the Northeast Chukchi shelf on the southern flank of Hanna Shoal (Fig. 1), the Chukchi Ecosystem Observatory (CEO), is a set of instrumented moorings that has been collecting high-resolution, continuous biological, biogeochemical, and physical measurements since 2014 (Danielson et al. 2017a, b; Hauri et al. 2018; Lalande et al. 2020). The CEO provides a unique opportunity to quantify biological and physical patterns over a continuum of temporal scales.

Continuous datasets derived from remote sensing technologies potentially fill data gaps identified above and provide data to characterize highly dynamic and rapidly changing high latitude ecosystems. In this study, we conduct a time-scale decomposition of biological metrics derived from acoustic backscatter and environmental variables to quantify temporal scales of variation (i.e. periodicities) in densities and vertical distributions of fish and zooplankton, and identify scale and time-dependent biological-physical associations using the CEO as a study case. Results from this study will improve our mechanistic understanding of ecosystem dynamics and constitute first steps towards an effective prediction and detection of biological responses to a rapidly changing environment.

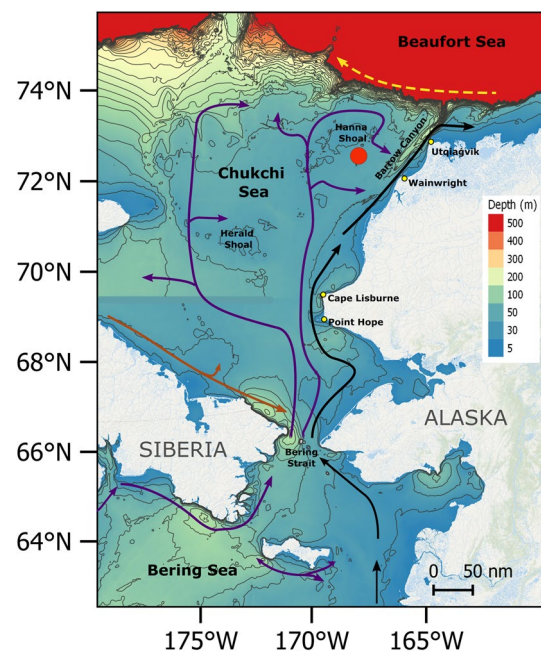


Fig. 1 Study region map with bathymetric depths, and main flow pathways. The yellow arrow represents the Beaufort Gyre, black arrows represent the Alaskan Coastal Current, the brown arrow represents the Siberian Coastal Current, and purple arrows represent pathways of Bering Shelf, Anadyr, and Chukchi shelf waters. The red circle indicates the location of the Chukchi Ecosystem Observatory

Methods

Study site

The CEO is located on the NE Chukchi Sea shelf between Hanna Shoal and Barrow Canyon (71°35.976'N, 161°31.621'W) at 46 m depth (Fig. 1). Located in the midst of a hotspot of benthic biomass (Grebmeier et al. 2015), the CEO area attracts populations of upper trophic level consumers (Jay et al. 2012; Hannay et al. 2013). The CEO seascape varies seasonally: a late fall and winter homogeneous water column with thickening sea ice and light-limited primary production (Weingartner et al. 2005), a spring with diatoms and sea ice algae blooms triggered by the return of light (Gradinger 2009; Arrigo et al. 2014), and a stratified, warmer, nutrient-rich water column after May when sea ice starts to melt, triggering massive phytoplankton blooms under the ice (Arrigo et al. 2012) and through the summer (Hill et al. 2018). In the fall, the intensification of winds and diminishing solar input allows the water column to re-homogenize and surface waters are replenished with nutrients that supports fall phytoplankton blooms until sunlight fades.

Environmental data

To examine biological-physical associations that vary over time and among temporal scales, we used physical environmental data collected at the CEO and supplemented it with data from other sources. Near-bottom and midwater salinity and temperature measurements were collected hourly at the CEO during the five deployment years using a Sea-Bird SBE-37 MicroCat located at a depth of 43 m (seafloor depth of 46 m) and a Sea-Bird Scientific SBE-16 SeaCat deployed at 28–33 m depth. Daily averages of satellite-based sea ice concentration (%) data were downloaded from the National Snow and Ice Data Center (NSIDC) archive (http://nsidc.org/data/seaice/pm.html#pm_seaice_conc) (Maslanik and Stroeve 1999). Hourly sun altitudes relative to the horizon at the CEO were calculated using the ‘sunAngle’ function of the R package *oce* (v. 1.3–0, Kelley and Richards 2021). Daily sunrise and sunset times were calculated using the ‘sunrise’ function of the R package *maptools* (v. 1.0–2, Bivand and Lewin-Koh 2019). Sun altitude and daylength were used as metrics of light irradiance. Daily maximum and minimum air temperatures recorded at the nearby coastal city of Utqiagvik were obtained from the U.S. climate data website (<https://www.usclimatedata.com/climate/barrow/alaska/united-states/usak0025>). Hourly wind speed and direction data for the CEO location were obtained from the Copernicus Climate Change Service (Hersbach et al. 2018).

Acoustic data acquisition

Active acoustic data were used to characterize temporal patterns in fish and zooplankton densities and behavior in the Chukchi Sea. Acoustic backscatter (i.e. ensemble reflected energy) data were collected using an ASL, Acoustic Zooplankton Fish Profiler (<http://www.aslenv.com/AZFP.html>), deployed at 28–35 m depth (depending on year), looking upwards (Fig. 1). The instrument operated at 38 (12°), 125 (8°), 200 (8°), and 455 (7°) kHz (nominal beam width, measured between half power points given in parenthesis) since September 9, 2014. The AZFP collected data every 15 s (0.067 Hz) at a vertical resolution of 4 cm. Every summer, a new mooring with a manufacturer-calibrated AZFP was deployed followed by the recovery of the previous mooring to ensure continuity of data collection.

Acoustic data processing and classification

Acoustic data from the CEO was processed using Echoview software (v. 9.0). Background noise was subtracted and a minimum signal-to-noise ratio filter of 6 dB re 1 m⁻¹ (hereafter dB) was applied. Echoes within 3 m from the face of the transducer were excluded from the analyses to avoid the integration of echoes in the acoustic nearfield. Sea water

surface and sea ice edges were delimited using Echoview’s linear offset operator algorithm followed by visual inspection and manual correction. A surface exclusion line was set 0.5 m below the corrected surface and echoes above the line were excluded to ensure that backscatter from surface turbulence or sea ice were not included in analyses.

We classified acoustic backscatter into fish and zooplankton categories using differences in mean volume backscattering strength (MVBS) (Madureira et al. 1993; Kang et al. 2002; Korneliussen and Ona 2003) between 125 and 38 kHz data ($\Delta MVBS_{125-38 \text{ kHz}}$). Backscatter measurements were averaged in four pings (1 min) horizontal by 1 m vertical cells for each frequency. Cells with $\Delta MVBS_{125-38 \text{ kHz}}$ values in the range of – 16 to 8 dB were classified as fish and $\Delta MVBS_{125-38 \text{ kHz}}$ values in the range of 8–30 dB were classified as zooplankton (cf. De Robertis et al. 2010). A minimum volume backscattering strength (Sv) integration threshold of – 70 dB was applied to the 38 kHz (“fish”) data (cf. De Robertis et al. 2017) and a – 80 dB Sv integration threshold was applied to the 125 kHz (“zooplankton”) data (cf. Ressler et al. 2012).

Although no direct fish and zooplankton sampling was conducted in association with acoustic measurements, we can rely on catch data from fisheries surveys carried out in the NE Chukchi Sea to attribute most of the observed fish backscatter to polar cod (*B. saida*). Polar cod accounted for 81–90% of total fish biomass and abundance from bottom (Barber et al. 1997; Goddard et al. 2014; Sigler et al. 2017; Logerwell et al. 2018) and pelagic (Lowry and Frost 1981; De Robertis et al. 2017) trawl surveys conducted in spring-fall ice-free seasons. From four midwater trawls conducted on Hanna Shoal in close proximity to the CEO in summer of 2017, Levine and De Robertis (*pers. comm*) observed that polar cod constituted the majority of the fish biomass and abundance. Other species occasionally caught included capelin (*Mallotus villosus*), *Lumpenus* spp, staghorn sculpin (*Gymnocanthus tricuspis*), and Liparidae snailfish. As further support of our backscatter categorization, age-0 polar cod was the dominant contributor to 38 kHz backscatter in the northern region of the Chukchi Sea in acoustic-trawl surveys conducted in 2012 and 2013 as part of the Arctic Ecosystem integrated survey (De Robertis et al. 2017).

Zooplankton communities in the Hanna Shoal area are dominated numerically by small copepods such as *Oithona similis* and *Pseudocalanus* spp. and in biomass by the larger *Calanus glacialis/marshallae* (Lane et al. 2008; Elliott et al. 2017; Lalande et al. 2020). The Arctic copepod *Calanus hyperboreus* has also been observed in this area (Lane et al. 2008; Hopcroft and Day 2013; Lalande et al. 2020). Other non-copepod groups that contribute to the Chukchi zooplankton community biomass, especially during summer, are the appendicularians *Fritillaria borealis* and *Oikopleura vanhoeffeni*, the chaetognath *Parasagitta elegans*, and some

meroplankton species, particularly bivalve, polychaete and echinoderm larvae (Hopcroft et al. 2010; Ashjian et al. 2017; Lalande et al. 2020).

Electric interference was visible in the 125 kHz data throughout most of the first deployment year (September 2014–August 2015) and as a result, the first year of data was excluded from further analyses. Fish and zooplankton Sv were integrated into hourly averages from September 1, 2015 to August 18, 2019 and used in all analyses.

Data analysis

Our analytic approach consists of characterizing temporal scales of variability in density and vertical distribution metrics for fish and zooplankton using wavelet analysis, describing scale- and time-dependent associations of these metrics with physical environmental variables using wavelet coherence, and assessing synchronicity and lags in biological-physical associations using phase angle differences between pairs of variables.

Characterization of biological vertical distributions

A suite of metrics derived from acoustic data, collectively referred to as Echometrics (Burgos and Horne 2008; Urmy et al. 2012), were used to quantify variations in density and vertical distributions of fish and zooplankton in the water column at the CEO. Echometrics can be used to efficiently summarize temporal variability in abundance and behavior in large datasets and to detect and quantify variability across a broad range of temporal scales (e.g. transient events, diel vertical migrations, and interannual changes). The Echometrics suite includes: (1) mean Sv (units: dB re m^{-1}), an index of organism mean density (MacLennan et al. 2002); (2) center of mass (units: m), the mean weighted location of backscatter in the water column relative to the bottom; (3) inertia (units: m^2), a measure of organism dispersion (i.e. variance) from the center of mass; and (4) an aggregation index (units: m^{-1}), which measures vertical patchiness of backscatter through the water column. The aggregation index is calculated over a scale from 0 to 1, with 0 being evenly distributed throughout the water column and 1 being aggregated.

Scales of variation in biological characteristics

To identify the dominant scales of temporal variability in fish and zooplankton metrics and to examine the consistency in dominant scales of variability through time we used wavelet analysis (Torrence and Compo 1998). A wavelet transform decomposes a time series across time and frequency domains through the convolution of a waveform—the wavelet—that is stretched or compressed (i.e. scaled) and

slid through the time series (i.e. translation). The result is a 2-dimensional heat-map, called a scalogram, that represents the wavelet power (i.e. variance) contributed by each temporal period (or scale) at each time step. Therefore, a wavelet transform allows not only the detection of constituent periods or frequencies (analogous to a Fourier Transform), but also the temporal location of frequency components within the record (Torrence and Compo 1998; Cazelles et al. 2008), which may temporally vary in phase.

A continuous Morlet mother wavelet function (Torrence and Compo 1998) was applied to each time series. Continuous wavelets enable the localization of transient patterns in variance and have been previously used for the analysis of temporally indexed acoustic data (e.g. Urmy 2012; Viehman and Zydlewski 2017; Gonzalez et al. 2019). Temporal scales analyzed ranged from two hours (twice the hourly aggregated data resolution) to 11,585 h (one third of the time series length). Wavelet power was calculated using the R package WaveletComp (v. 1.1, Roesch and Schmidbauer 2018). Statistical significance in localized wavelet power was evaluated through comparison to a white noise (constant value, equal to the time series variance) null hypothesis at a 95% confidence level (Torrence and Compo 1998) using 100 simulations. Edge effects were minimized by adding zeroes at the beginning and end of each data series to increase the total length of the series to the next power of two (Torrence and Compo 1998).

Horizontal integration of wavelet power at each scale over the entire deployment—the global wavelet spectrum—allows the measurement of variance contributed by each scale across the entire series. The global wavelet spectrum was calculated using the R package WaveletComp (v. 1.1, Roesch and Schmidbauer 2018). Significance of this time-averaged variance was tested against white noise at a 95% confidence level (Torrence and Compo 1998).

Time- and scale-dependent biological and physical associations

To assess time and scale-dependent correlations between biological metrics and the marine environment we used wavelet coherency. Wavelet coherency measures the correlation (taking values from 0 to 1) and phase (values from $-\pi$ to π) of two variables at each time step and scale of the decomposed series enabling the description of localized (in scale and time) and lead-lag relationships between two time series (Torrence and Compo 1998). Daily averages of all variables were used to compute wavelet coherencies between the four biological metrics and physical variables. Daily values correspond to the highest common temporal resolution for all biological and physical variables. The R package WaveletComp (v. 1.1, Roesch and Schmidbauer 2018) was used to calculate wavelet coherence and phase. Statistical

significance of localized wavelet coherency between each pair of variables was also tested against white noise using 100 simulations at a 95% confidence level. Global wavelet (i.e. time averaged) coherence was calculated and its significance was tested against white noise at a 95% confidence level (Torrence and Compo 1998). To look at potential predator–prey interactions between fish and zooplankton communities we calculated wavelet coherence between hourly series of fish and zooplankton densities (i.e. mean Sv).

Results

Echometrics and environmental conditions

Densities and vertical distributions of fish and zooplankton displayed intra-annual temporal variability (Fig. 2). Seasonal patterns were observed in all metrics for both backscatter groups. Backscatter corresponding to fish and zooplankton was observed throughout the year with greater densities (i.e. mean Sv) in summer than in winter. Peak densities of fish were observed in July–September and highest densities of zooplankton were recorded in August–November (Fig. 2a). In general, fish were located deeper in the water column than zooplankton. Both backscatter groups were located deeper

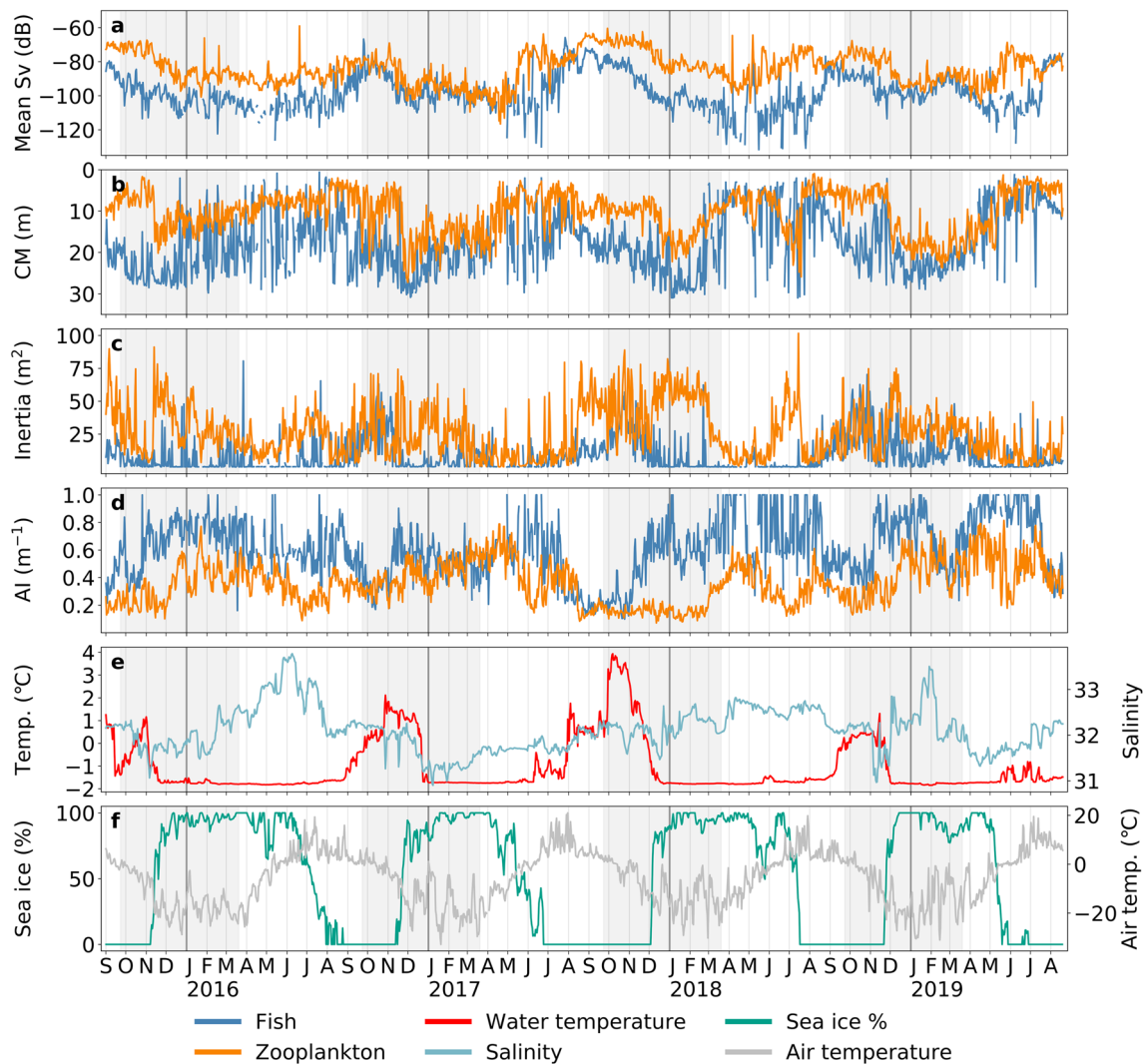


Fig. 2 Daily averages of fish and zooplankton density and vertical distributions derived from acoustic backscatter data (a–d), and physical variables (e, f) at the Chukchi Ecosystem Observatory from September 1, 2015 to August 18, 2019. *CM* center of mass, *AI* aggrega-

tion index. Shaded areas highlight months between Fall and Spring equinoxes. Water temperature and salinity values correspond to mid-water measurements and air temperature is represented by minimum daily values

in the water column during winter and started ascending around February, reaching depths closest to the surface by the end of the summer (i.e. late August–September) and then descended to deeper waters (Fig. 2b). Fish dispersion (i.e. inertia) was relatively low throughout the year with highest values observed in autumn. Zooplankton dispersion was higher in autumn and winter months except for 2018 when high dispersion of organisms located deeper in the water column was also observed in June–July (Fig. 2c). Fish and zooplankton were more strongly aggregated in winter or spring months while weaker aggregations were observed in autumn each year (Fig. 2d). Short-period (24 h or less) variability was also present in the data, with high hourly variability observed in all metrics (not shown).

Inter-annual variability was observed in the timing and amplitude of seasonal changes. For example, the peak in fish and zooplankton production was much higher and more extended during late summer–early fall of 2017 (Fig. 2a). This high production was coincident with the highest water temperatures recorded in 2017 (Fig. 2e). The timing of the peaks in fish and zooplankton density was different each year (Fig. 2a). Peaks in fish density shifted from late September in 2016, to late July in 2017, and to May and late August in 2018 whereas peaks in zooplankton were observed in November in 2016, September in 2017, and August in 2018 (Fig. 2a).

We observed seasonal and inter-annual variations in sea ice concentration, air and midwater temperature, and salinity (Fig. 2e, f). Midwater temperatures remained above 0 °C during October–December in 2016, from August 2016 to January 2017 and during October–November in 2018 with 2017 being the warmest in the series with midwater temperatures reaching 4 °C by October (Fig. 2e). Midwater salinity values were lowest (ca. 31) in November each year with the exception of 2017 when lowest values were recorded in January (Fig. 2e). Sea ice started to concentrate in November each year reaching 100% concentrations in December–January (Fig. 2f). Sea ice melt started in June in 2016 and in May in 2017–2019, although sea ice cover remained present until July in 2016 and 2018 (Fig. 2f). Minimum air temperatures remained above 0 °C from May–June to October each year (Fig. 2f).

Dominant scales of temporal variability in biological metrics and their consistency through time

Variability in biological characteristics at the CEO was observed at multiple temporal scales (i.e. periods) with varying degrees of consistency through time (Figs. 3, 4). Variability in fish metrics (Fig. 3) was concentrated at the ~1-year period (~8679 h), indicating a strong signal of intra-annual variations in fish densities and vertical distributions. A consistent band of high wavelet power was observed around a

4096-h period (ca. 5.5–6 months) and was represented as a peak in the global wavelet plots. This peak in wavelet power at the ~6-month period was present in all metrics, but this signal was much weaker for the aggregation index (Fig. 3d). Variability at this scale, although present throughout the year, was more pronounced in summer months (Fig. 3). A third peak in average wavelet power was observed at a ~24-h period representing diel changes in fish metrics. The occurrence of the 24-h period signal was less consistent through time than annual and ~6-month periods but the strength of the signal (i.e. wavelet power) was high when present (Fig. 3a). For aggregation index, the ~24-h period wavelet power was particularly accentuated in 2019, compared to previous years (Fig. 3d). High wavelet power values localized at specific times within the series were observed in the scalograms and as smaller peaks in global wavelet spectra at 2435-h (~3 months), 683-h (~28 days), and 341-h (~14 days) periods for mean Sv, center of mass, and inertia (Fig. 3a–c). Variability at these time scales was stronger from late fall to early spring each year (Fig. 3a–c). For inertia, wavelet power was noticeably high around the ~3-month period from July to March with some variations in temporal extent among years (Fig. 3c).

Variability in zooplankton metrics was also concentrated in three main scales with peaks at the ~1-year and ~24-h periods, matching observations for fish, and at the 2896-h (~4 months) period (Fig. 4) with a few exceptions. For the aggregation index, the local peak observed at the 1-year period for all other metrics was not present but a peak in the average wavelet power spectra occurred at a 9-month period (Fig. 4d). For zooplankton center of mass, a peak occurred at the ~5.5-month period instead of the ~4-month period that was observed for all other metrics and an additional peak was observed at the 1933-h (~3 months) period (Fig. 4b). Variability at the 574-h (~28 days) and 341-h (~14 days) periods was observed for all metrics during November–June and were represented as small peaks in the average wavelet power spectra (Fig. 4). These two scales of temporal variability suggest monthly and fortnightly influences of moon cycles on zooplankton density and vertical distribution through the modulation of tides and light in winter months. Variability at an 80-h (~3 days) period was also observed during September–November for center of mass and inertia in both fish and zooplankton groups each year (Figs. 3b–c, 4b–c). This peak is attributed to the occurrence of storms that are typically accentuated in fall.

In summary, variability in biological metrics occurred over time scales with peaks in average wavelet power observed crossing more than 3 orders of magnitude in time at the annual, seasonal (~3–6 months) and diel (~24-h) periods. Smaller but still significant peaks resulting from a less consistent presence throughout the series were observed at intermediate time scales of 3–28 days.

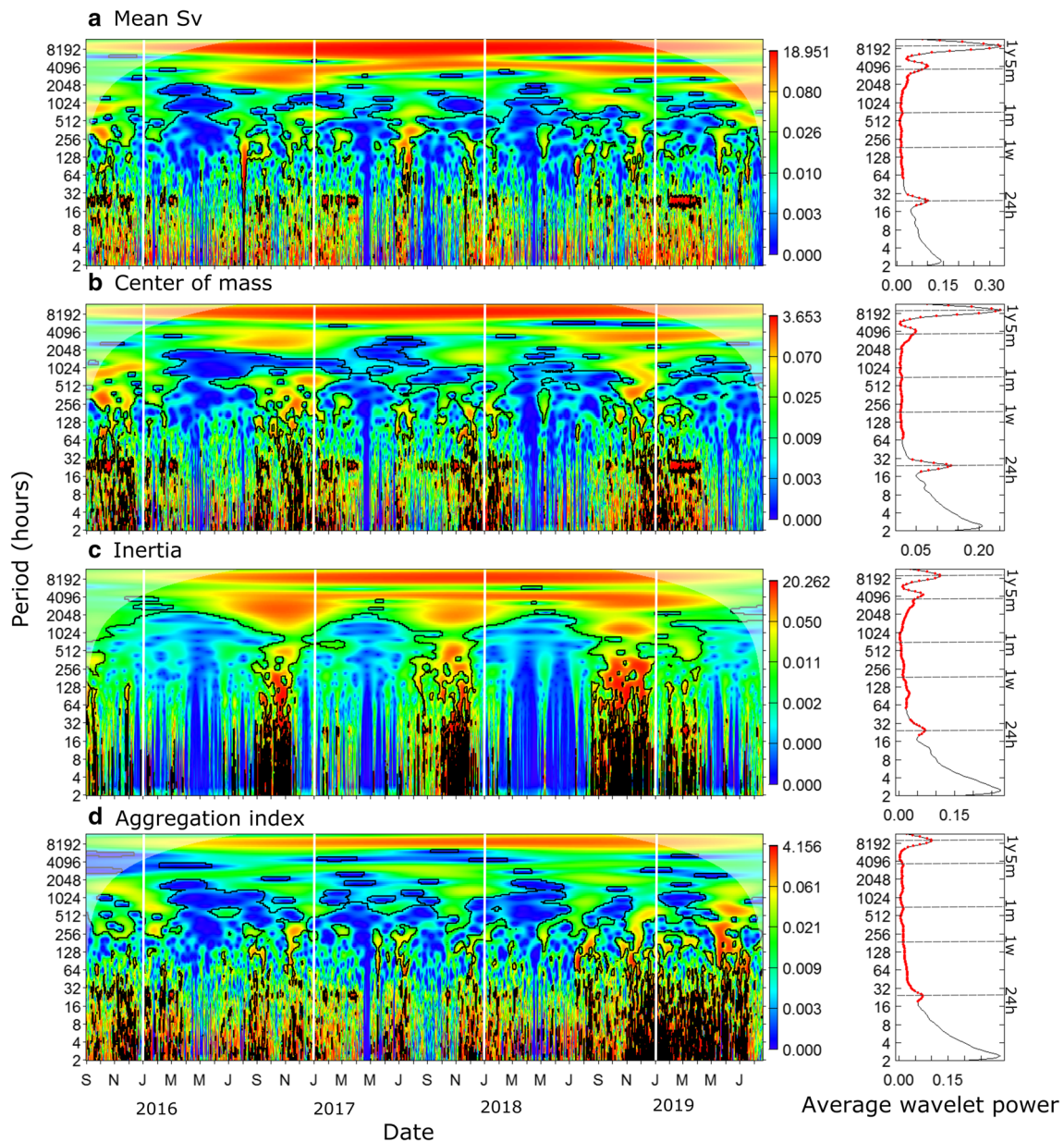


Fig. 3 Time-scale decomposition of hourly values of fish density and vertical distribution metrics derived from acoustic backscatter at the CEO: **a** Mean Sv, **b** center of mass, **c** inertia, **d** aggregation index. The color bar represents the wavelet power (σ^2). The shaded area represents the cone of influence (edge effects) and the black

contour lines indicate areas of significance (95% confidence against white noise). Time averaged wavelet power (global wavelet spectrum) is shown on the right for each metric. Significant periods (95% confidence against white noise) are shown in red. Dashed lines indicate 1-year, 5-month, 1-month, 1-week, 24-h periods

Predator–prey associations

Coherence between fish and zooplankton densities was observed at multiple temporal scales with variations in lagging variable at each scale (Fig. 5). A peak in average wavelet coherence between groups was observed at a 1-year period. At this period, a significant positive association was observed throughout the entire deployment led by zooplankton (Fig. 5) with phase differences (i.e. fish

phase—zooplankton phase, hereafter phase) of -0.2 rad (~ -11 days) to -0.4 rad (~ -23 days). Significant, positive associations at 2.5-month, 1-month, and 11-day periods were observed in winter and spring months each year with fish (mean phase: $+1.6$ rad or $+19$ days), zooplankton (mean phase: -0.6 rad or -3 days), and fish (mean phase: $+0.3$ rad or $+12$ h) as the leading variables (Fig. 5), respectively. Significant coherence between both groups was also observed at the diel scale (Fig. 5).

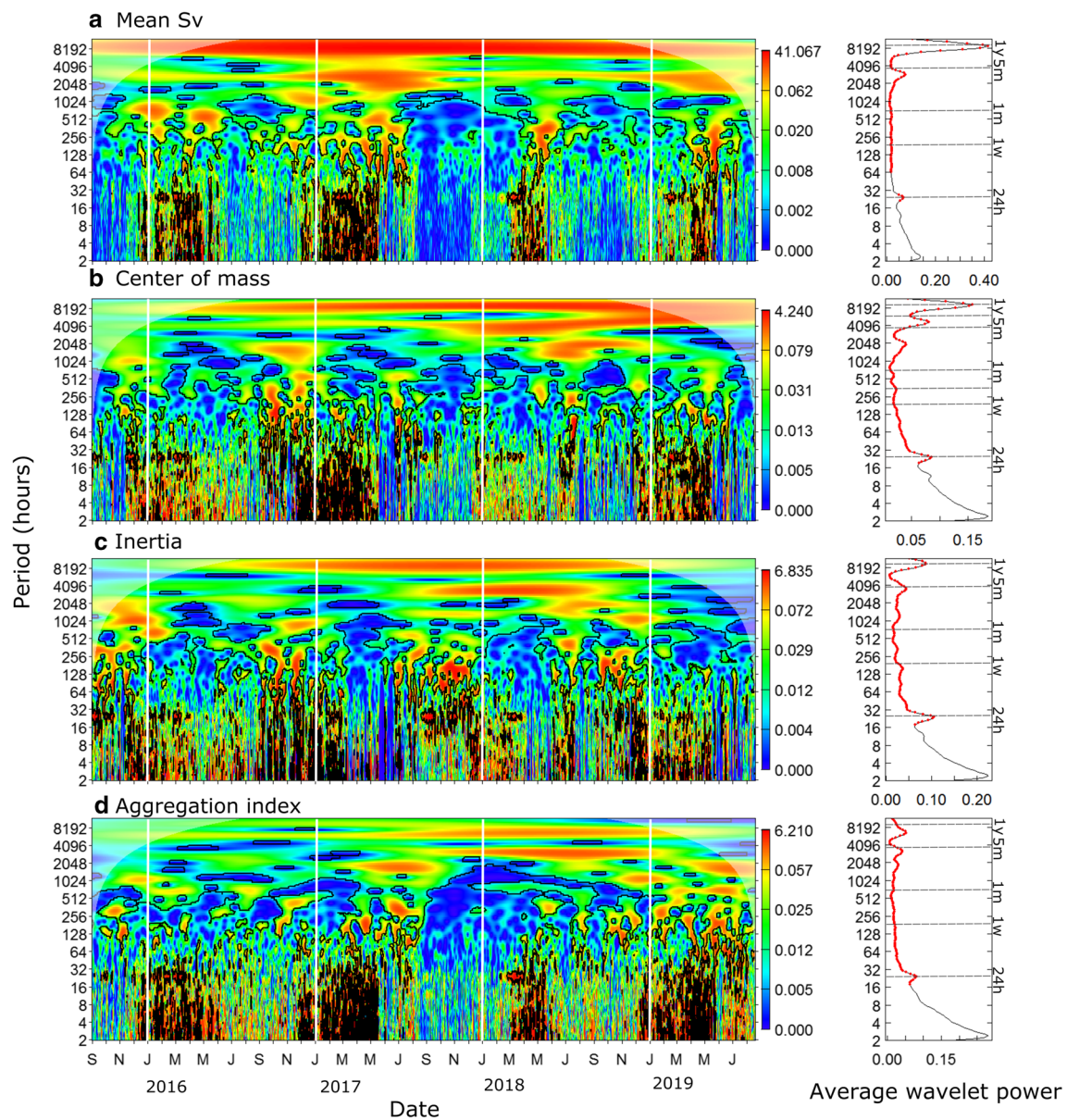


Fig. 4 Time-scale decomposition of hourly values of zooplankton density and vertical distribution metrics derived from acoustic backscatter at the CEO: **a** Mean Sv, **b** center of mass, **c** inertia, **d** aggregation index. The color bar represents the wavelet power (σ^2). The shaded area represents the cone of influence (edge effects) and the

black contour lines indicate areas of significance (95% confidence against white noise). Time averaged wavelet power (global wavelet spectrum) is shown on the right for each metric. Significant periods (95% confidence against white noise) are shown in red. Dashed lines indicate 1-year, 5-month, 1-month, 1-week, 24-h periods

Scale and time-dependent coherence among biological metrics and physical environment

Strength of bio-physical associations varied between backscatter groups, among biological metrics, and among temporal scales of variation (Figs. 6, 7). Significant biological-physical associations presented in this section result from consistently significant coherence throughout

the entire time series and can therefore be considered as robust associations. Only biological-physical associations occurring at time scales identified as dominant scales of temporal variability in biological metrics in “Dominant scales of temporal variability in biological metrics and their consistency through time” section (i.e. peaks in metrics global wavelet spectra) are described here and further discussed in the “Discussion” section.

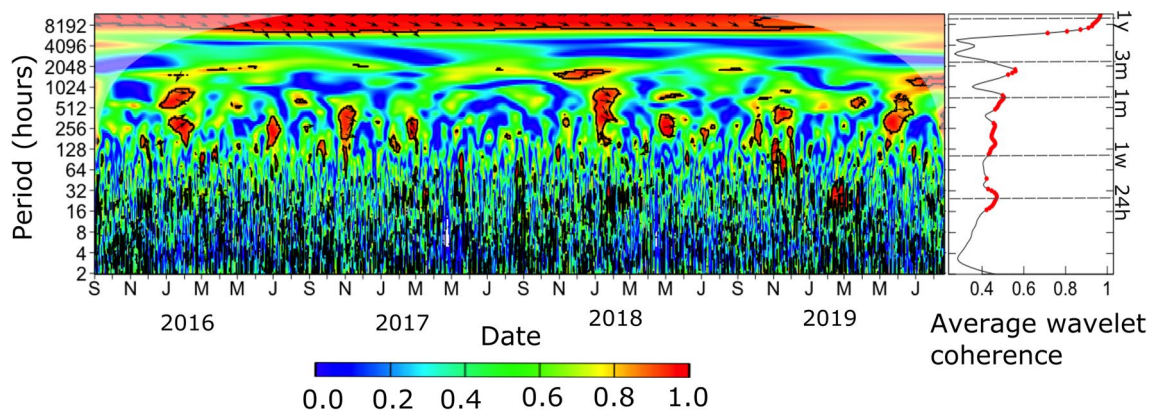


Fig. 5 Wavelet coherence between hourly values of fish and zooplankton density (mean volume backscattering strength). The color bar represents the wavelet coherence. The shaded area represents the cone of influence (edge effects) and the areas of significance are traced with a black line (95% confidence against white noise). Arrows indicate the phase difference between the two variables of the wave-

let spectra (right arrows indicate series are in phase, left arrows indicate series are completely out of phase (180°), and an arrow pointing vertically upward means the second series lags the first by 90°). Time averaged wavelet coherence is shown on the right with significant periods (95% confidence against white noise) shown in red. Dashed lines indicate 1-year, 3-month, 1-month, 1-week, 24-h periods

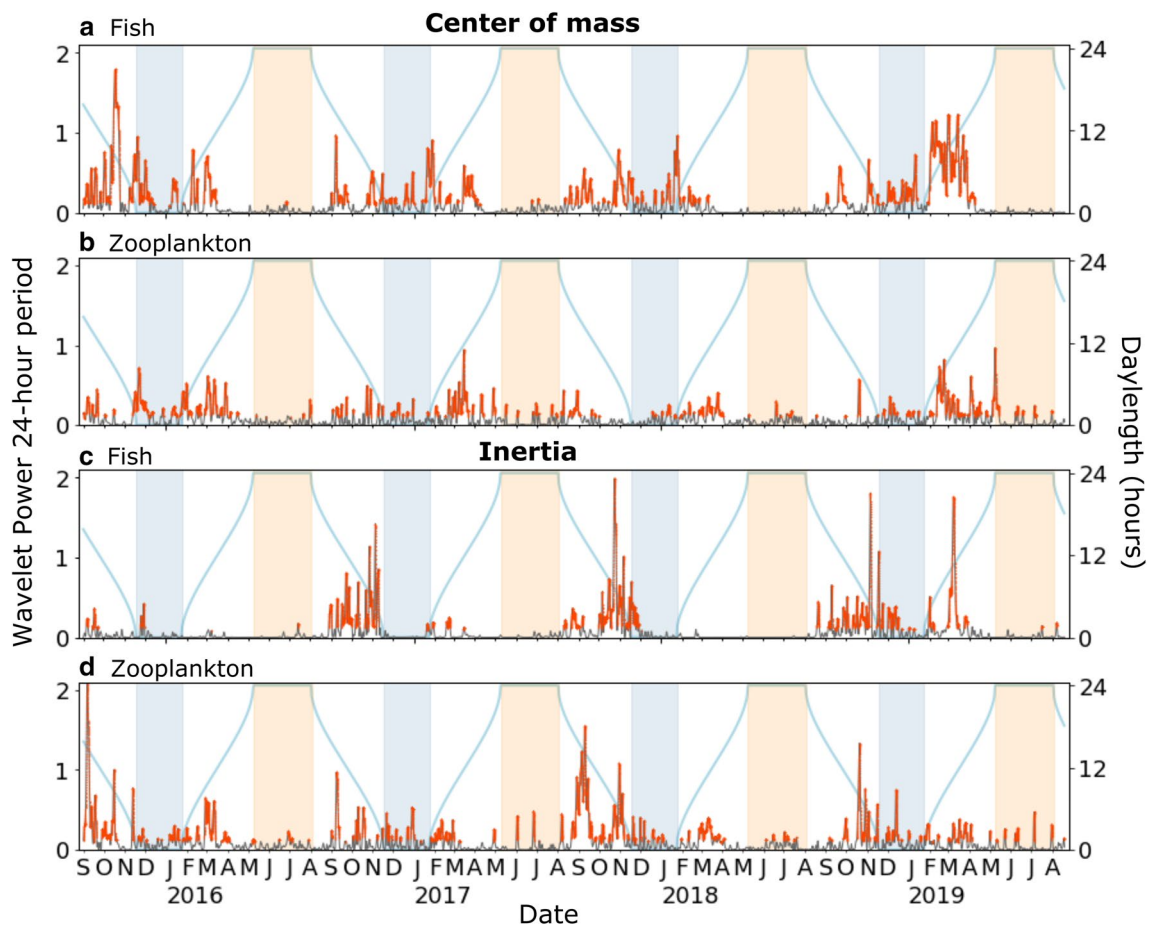


Fig. 6 Temporal variation in the strength of the 24 h-period signal in center of mass (**a, b**) and inertia (**c, d**) for fish (**a, c**) and zooplankton (**b, d**) in association with daylength at the Chukchi Ecosystem Obser-

vatory. Significant peaks in wavelet power are shown in red. Shaded areas in orange and blue indicate periods of midnight sun and polar night, respectively

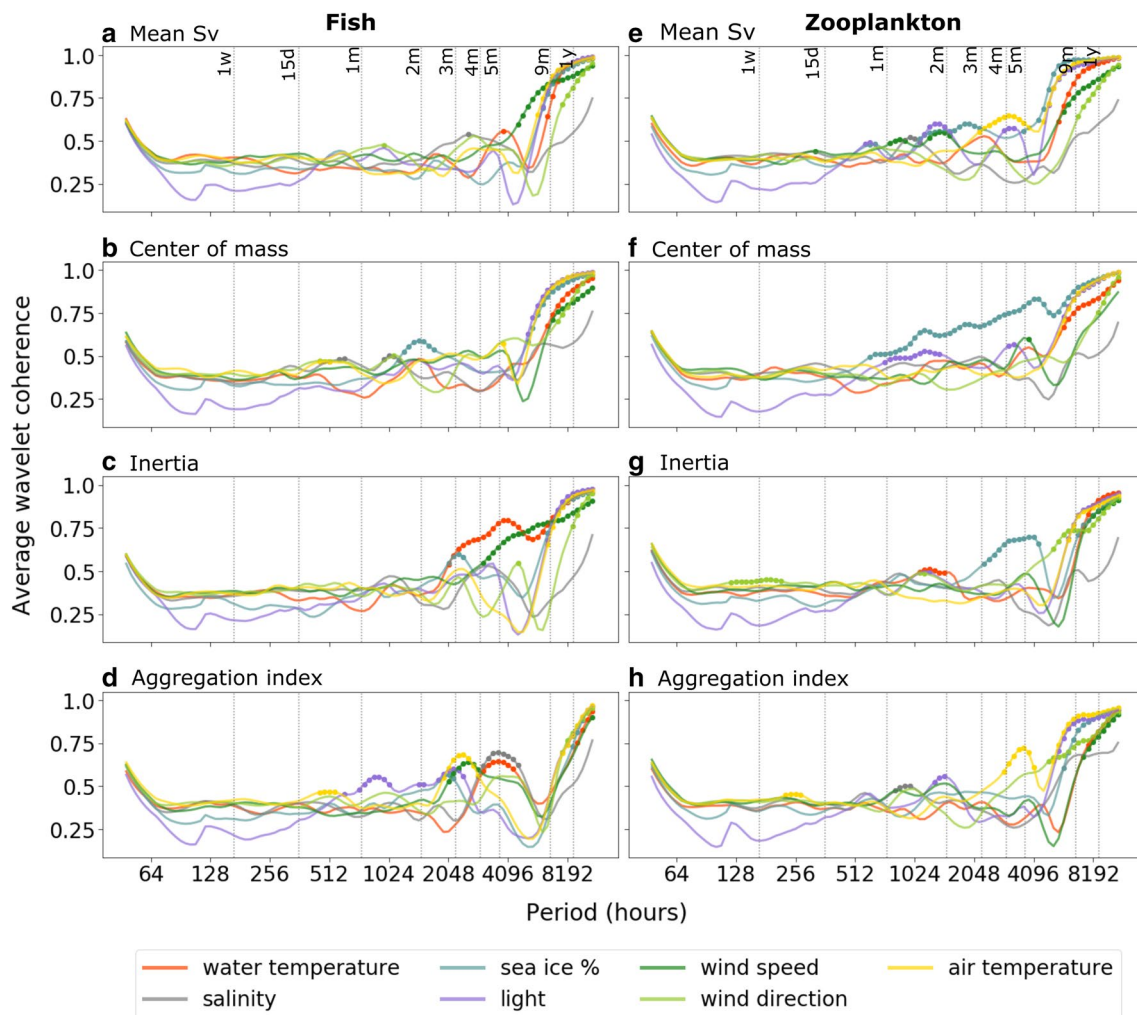


Fig. 7 Average wavelet coherence between daily values of fish (a–d) and zooplankton (e–h) density and vertical distribution metrics derived from acoustic backscatter and physical environmental variables at the CEO. Circles represent significant values at the 95% confidence. Water temperature corresponds to midwater temperature, air

temperature to minimum air temperature, and light corresponds to sun altitude. Bottom salinity is shown for fish and midwater salinity is shown for zooplankton. Dotted lines indicate periods of 1 week, 15 days, 1–5 months, 9 months, and 1 year

Diel variability

The strength of the 24-h period signal in fish and zooplankton location and dispersion (i.e. center of mass and inertia) in the water column, indicative of diel vertical migrations (DVM), varied throughout the year (Fig. 6). In general, highest peaks in the strength of the diel signal in both metrics occurred at intermediate daylengths (i.e. autumn and spring) for both fish and zooplankton. In particular, diel cycles in center of mass for both backscatter groups were stronger during autumn and spring months each year but did persist with lower values throughout winter months. From March to September this signal was non-significant for fish and was low or non-significant for zooplankton (Fig. 6a, b).

The diel signal in fish dispersion was typically strongest during late summer and autumn months, with highest

wavelet power values observed in November when there are ~5 h of daylight at the CEO site (Fig. 6c). Significant values of the diel signal in fish inertia were also observed in February–March in 2017 and 2019 (Fig. 6c). Diel cycles in zooplankton dispersion were more persistent throughout the year, with lower but still statistically significant values during both midnight sun (i.e. 24 h of daylight) and polar night (i.e. 0 h of daylight) months (Fig. 6d). Annually, the highest values in wavelet power of the 24-h period for zooplankton dispersion were observed in September–November (Fig. 6d). The observed association between patterns in vertical distribution metrics at the DVM period and light (daylength) patterns was supported by high significant coherence between hourly values of fish and zooplankton metrics, and sun altitude around the 24-h period (Online Resource 1).

Multi-day to monthly variability

At the ~1-month scale, we found significant associations between echometrics and light, salinity, and wind. In particular, fish mean Sv and center of mass were associated with wind direction, while fish aggregation index was associated with light irradiance patterns (Fig. 7a–d). For zooplankton, patterns in mean Sv and center of mass were associated with wind and light irradiance patterns. (Fig. 7e–h). At this scale, water salinity was associated with fish center of mass, and density and patchiness of zooplankton (Fig. 7). Biological associations with wind patterns were tighter in autumn when storms are stronger and more frequent. Associations with salinity were stronger in autumn and spring months, typically October–November and April–May (Online Resource 2) potentially associated with periods of sea-ice formation and melt.

Patterns in zooplankton mean Sv and aggregation index observed at the ~14-day period were associated with wind speed and minimum air temperature, respectively (Fig. 7e, h), whereas no significant associations were observed for fish metrics at this scale (Fig. 7a–d). At the ~6-day period midwater salinity and wind direction were associated with the fish aggregation index and zooplankton inertia (Fig. 7d, g). Peaks in variance observed between 1 and 3-day periods in fish and zooplankton location and dispersion in the water column (i.e. center of mass and inertia) could not be associated with any environmental variables (Fig. 7).

Seasonal and annual variability

Variability in biological metrics at scales ranging from 3 to ~6 months was associated with distinct environmental covariates and potentially reflects differences in seasonality among physical drivers. Covariates associated with biological metrics at each of these periods varied between fish and zooplankton (Fig. 7, Online Resource 2). For fish, significant coherence at the ~3-month period was observed between mean Sv and bottom salinity, and between inertia and sun altitude. No significant associations were found for center of mass (Fig. 7a–d). For zooplankton, significant coherence at a 3-month period was present between mean Sv, center of mass, inertia, and sea ice concentration (Fig. 7e–h).

High variance at the ~5.5-month time scale observed in fish metrics (mainly mean Sv, center of mass, and inertia, Fig. 3a–c) was associated with water and air temperature (Fig. 7e–g). Water temperature values that remain at the freezing point half of the year (October–April) undergo warming-cooling cycles over a period of ~5 months. Water temperature starts to increase in June–July, reaches maximum values in August–September, and returns to minimum values by October–November (Fig. 2e). Biological variability shifted from a time scale of ~5.5 months in 2015, 2016,

and 2018 to ~6 months in 2017 (Fig. 3) coinciding with temperatures remaining relatively high for an extended period of time in summer of 2017 (Fig. 2e). In particular, we observed that coherence between fish mean Sv and water temperature was highest from October to February each year and was particularly strong in 2017. Significant, in-phase associations between water temperature and fish dispersion were present through April 2016–February 2017 and September 2017–February 2019 whereas significant, out-of-phase associations with the aggregation index were present only during 2018 (Online Resource 2). Significant associations were also observed with wind speed during fall and winter months each year (November 2016–January 2017 and October 2018–April 2019) when stronger winds enhance mixing of the water column. For zooplankton, variance in the center of mass at this scale (Fig. 4b) was not associated with temperature but with fluctuations in sea ice concentration and wind speed (Fig. 7f). This association between center of mass and sea ice concentration was present throughout the time series except for January–October 2017 and January–August 2019 when significant, out-of-phase coherence with light irradiance was observed (Table 1, Online Resource 2).

Variability observed at the ~4-month time scale in zooplankton mean Sv (Fig. 4a) was associated with air temperature and light irradiance (Fig. 7e) whereas 4-month cycles in inertia (Fig. 4c) were associated with temporal patterns in sea ice concentration (Fig. 7g). These associations were present throughout the year although stronger in October 2016–September 2017 and again from October of 2018 until the end of the time series. For fish, significant coherence at a ~4-month period between mean Sv and bottom salinity were only observed during summer months with both variables out of phase (Table 1, Online Resource 2).

At the largest time scale (i.e. ~1-year period), all biological metrics of both backscatter groups were associated with all physical variables except for salinity (Fig. 7). This observation is consistent with weak annual cycles observed in the salinity time series (Fig. 2e). At the ~1-year period, significant associations were consistent through time, except for wind speed where coherence with fish and zooplankton metrics decreased to non-significant values in January 2018 (Online Resource 2). Sea ice concentration was out of phase with mean Sv and inertia and in phase with center of mass for both backscatter groups at the annual scale. Minimum densities and dispersion of organisms located deeper in the water column were associated with highest sea ice concentrations in winter months (Fig. 2e, Online Resource 2). Water temperature was in phase with mean Sv and inertia (Table 1). Highest densities of highly dispersed organisms were recorded around October each year associated with warmest waters (Fig. 2e). Light irradiance and wind direction led fish and zooplankton densities by ~90°, whereas the two variables were out of phase with center of mass

Table 1 Summary table indicating presence (colored cells) of each of the scales of variability in metrics for fish (blue) and zooplankton (orange)

		Fish				Zooplankton			
		Sv	Cm	In	Ai	Sv	Cm	In	Ai
Annual	~ 1 year								
	MW temperature	+	+	+	-	+	+	+	-
	Air temperature	+	-	+	-	+	-	-	-
	Sea ice %	-	-	-	+	-	+	-	+
	Sun altitude	-	-	-	-	-	-	-	+
	Wind speed	+	+	+	-	+	-	+	-
	Wind direction	-	-	-	+	-	-	-	+
	~ 9 months								
	Air temperature								-
	Sea ice %								+
Seasonal	~ 5 months								
	MW temperature	+		+					
	Air temperature		-						
	Sea ice %						+		
	Wind speed						+		
	Wind direction				-				
	~ 4 months								
	Air temp.					+			
	Sea ice %								+
	Sun altitude					-			
Intermediate	~ 3 months								
	Sea ice %								+
	Sun altitude				+				
	Bottom salinity	-							
	~ 2 months								
	~ 28 days								
	Sea ice %								+
	Sun altitude				+	-	-	-	
	Wind speed					+			
	Wind direction	+	+					+	
Diel	MW salinity					+		+	
	Bottom salinity		+						
	~ 14 days								
	Air temperature								-
	Wind speed					+			
	~ 6 days								
	~ 3 days								
	~ 24 h								

Only dominant scales identified in “Dominant scales of temporal variability in biological metrics and their consistency through time” section are included here. Associations described here occur at or in the proximity to the indicated time scale. When present, significant associations between metrics and environmental variables at each scale are represented using + or - depending if the variables are in phase or out of phase, respectively

Sv mean Sv, Cm center of mass, In inertia, Ai aggregation index, MW midwater

(Table 1). The largest scale of variation in the zooplankton aggregation index, observed at a ~9-month period (Fig. 4d), was associated with patterns in air temperature, sea ice concentration, light irradiance, and wind direction (Fig. 7h).

In summary, despite the shallow depths of the CEO and the lack of changes in light intensity during polar night and midnight sun, fish and zooplankton displayed DVM throughout most of the year. Water temperature, sea ice concentration, and light radiation patterns tended to be the most important environmental factors associated with biological

metrics at the longest time scales. Salinity and wind patterns were important at seasonal-related (time scales ranging from ~3 to 6 months), and intermediate (~3–28 days) scales. Sea ice concentration was strongly associated with zooplankton metrics at time scales from 28 days to one year, while its association with fish metrics was only significant at the annual scale. Wind speed and direction were sporadically associated with biological metrics over a broad range (6 days–1 year) of time scales.

Discussion

In this study, focused on a high latitude marine ecosystem, we used multi-year abundance and behavior metrics of pelagic fish, zooplankton, and environmental covariates to identify scales of temporal variability. We observed that (1) variability in biological characteristics occurs at multiple temporal scales, (2) the relative importance of scale-dependent patterns in biological metrics varies through time, (3) coherence between environmental factors and biological metrics is scale-dependent, and (4) the strength of those biological-physical associations varies through time.

Diel variability and predator–prey associations

A strong diel signal (i.e. variability at a 24-h period) was observed in all metrics and backscatter groups. Diel variations in the vertical distribution of fish and zooplankton densities have been well described in many aquatic systems (Hays 2003; Cohen and Forward 2009). DVM is thought to be an evolved response to limited food at depth and avoidance of visual predators in shallow waters (Hays 2003). These vertical movements typically involve the upward migration of organisms to feed in surface waters at night and movements to depth to seek refuge from visual predators during the day, all cued by changes in light irradiance (Cohen and Forward 2009). In high latitudes, DVM have been observed during fall and spring, when pronounced day-night cycles are present (Falk-Petersen et al. 2008; Gjelland et al. 2009; Darnis et al. 2017). Despite the shallow depth at the CEO site, we observed fish and zooplankton DVM throughout most of the year, with the diel signal strongest during fall and spring.

A growing body of studies have shown that organisms respond to subtle changes in background light in the dark winter (Berge et al. 2009; Cohen et al. 2015; Hobbs et al. 2018). At the CEO, DVM by both fish and zooplankton persisted through the polar night (November–January), with the signal more pronounced in fish. Age-0 polar cod is the most abundant species in the NE Chukchi Sea during summer (De Robertis et al. 2017) and can also be reasonably expected to be dominant under the sea ice in winter.

Benoit et al. (2010) reported that young polar cod undergo DVM from December to May (beginning of midnight sun) possibly to avoid feeding interference with adult polar cod that remain at depth in the Beaufort Sea. For zooplankton, weakening of the DVM signal during winter could be a result of decreases in zooplankton abundances combined with the presence of both migrant and non-migrant zooplankton species in the CEO's winter assemblage. In winter, high abundances of *O. similis* copepods and lower abundances of stage five copepodites of *C. glacialis* were observed in sediment trap samples obtained at the CEO (Lalande et al. 2020). *O. similis* has been reported to perform small scale DVM in the Arctic (Ashjian et al. 2003; Daase and Falk-Petersen 2016) whereas stage five copepodites of *C. glacialis* enter diapause to overwinter at depth (Falk-Petersen et al. 2009; Elliott et al. 2017) and would not contribute to an acoustically-detected DVM signal in winter.

Occurrence of zooplankton DVM during midnight sun has been variable among study sites (Fortier et al. 2001; Blachowiak-Samolyk et al. 2006; Cottier et al. 2006; Wallace et al. 2010) suggesting that local characteristics (e.g. species composition, presence/absence of sea ice, and prey distribution) influence the occurrence and strength of DVM. Coarse temporal and vertical depth resolution of previous studies could be failing to detect DVM that occurred over a shorter duration and vertical distance in summer (Daase and Falk-Petersen 2016). At the CEO during midnight sun (May–August), the diel signal was absent for fish but present with minimal but significant strength for zooplankton. Benoit et al. (2010) reported a lack of synchronized movements of polar cod during midnight sun but the authors suggest that short individual (unsynchronized) migrations were possible. In this period of continuous light irradiance, polar cod and other planktivorous fish use shoaling in surface layers as an alternative or complementary strategy for predation avoidance (Gjelland et al. 2009; Matley et al. 2012). DVM persistence for zooplankton in May–June could be attributed to the presence of sea ice and phytoplankton aggregations at the CEO. Sea ice and dense phytoplankton layers that often occur near the subsurface pycnocline could attenuate light in the water column and provide these smaller (and less visible) organisms refuge from visual predators for a longer period of time (Lorenzen 1972; Wallace et al. 2010). Fortier et al. (2001) observed that herbivorous copepods *C. hyperboreus*, *C. glacialis*, and *Pseudocalanus acuspes* displayed normal DVM under ice despite the midnight sun in Barrow Strait. Once sea ice melts, the lack of light attenuation and increased phytoplankton availability as food throughout the water column could make zooplankton DVM unnecessary (Blachowiak-Samolyk et al. 2006), limited to a part of the population (Dale and Kaartvedt 2000), or become unsynchronized (Cottier et al. 2006).

At the diel scale, we observed co-variations in fish and zooplankton densities, which were accentuated around March. We cannot determine if this co-variation is a result of fish chasing their zooplankton prey or an avoidance response to their own visual predators. Supporting the latter, DVM patterns displayed by polar cod under ice in the Beaufort Sea were associated with the presence of ringed seals (Benoit et al. 2010), a known predator of polar cod (Born et al. 2004). Synchronicity between zooplankton and fish was also observed at an annual scale. Fluctuations in organisms' densities occur throughout the year, with densities increasing from late spring to early autumn due to increased local production and arrival of organisms from the Bering Sea (Kitamura et al. 2017). At the annual scale zooplankton was leading in phase, indicating a faster response to changes in the environment than fish throughout the year. Densities of fish and their zooplanktonic prey were synchronized at several other intermediate temporal scales, mainly during winter months. High coherence of fish and zooplankton abundance in winter could be attributed to the overall reduction of organisms in the region during this season rather than to an interaction between predators and their prey. Even though we provide feasible interpretations for strong covariations in fish and zooplankton densities there are caveats that need to be considered. First, fish and zooplankton density estimates are not independent, and we could expect some bias caused by a misclassification of fish and/or zooplankton acoustic backscatter. Second, acoustic backscatter classified as zooplankton represents a species assemblage. Fish, predominantly age-0 polar cod, could be preying on a subset of zooplankton species or on smaller zooplankton that were excluded in this study. Third, covariations between predator and prey could be generated by a common response of fish and zooplankton to a single or a combination of environmental drivers operating at a similar scale, rather than by a true interaction between predators and prey.

Multi-day to monthly variability

Cyclic extrinsic (e.g. moon phase) or intrinsic (e.g. hunger-satiation) cues can shape patterns in fish and zooplankton biomass distributions at temporal scales ranging from days to several weeks (e.g. Campbell et al. 2008; Berge et al. 2015; Last et al. 2016). Variability in fish and zooplankton vertical distributions observed at ~28-day and ~14-day periods from late fall to early spring could be associated with lunar and semi lunar cycles. During polar night, the moon is the dominant source of ambient light and may facilitate visual predation during winter (Berge et al. 2015). Last et al. (2016) observed that zooplankton sink to deeper waters every 29.5 days in winter coincident with periods of the full moon in the lunar cycle. Marine species can synchronize their distribution and behavior to the semi-lunar cycle,

which is coincident with full or new moon phases (Berge et al. 2015).

Periodicities of 4–12 days in fish center of mass observed during winter at the CEO could be a result of hibernation cycles interrupted by short feeding excursions by small polar cod. During winter in the Southern Ocean, Campbell et al. (2008) observed that *Notothenia coriiceps* enters a state of dormancy interrupted by awakenings of a few hours every 4–12 days. Benoit et al. (2010) suggested that polar cod could also be undergoing dormant-wake cycles in the Beaufort Sea during winter.

Temporal patterns in salinity and wind were also associated with fish and zooplankton density and vertical distribution metrics at scales of 6–28 days. Wind direction and strength affect properties of Chukchi shelf waters through changes in circulation or stratification/mixing of the water column in summer and fall (Weingartner et al. 2013; Danielson et al. 2017a). In autumn, enhanced mixing by strong wind events can re-nourish depleted surface waters with nutrients from below the stratified layer, triggering a phytoplankton bloom (Lin 2012; Zhao et al. 2015) with cascading effects to higher trophic levels (Fujiwara et al. 2018). Changes in salinity, that are associated with changes in water masses and sea ice cycles, have also been reported to influence species' distributions in the Pacific Arctic (e.g. Norcross et al. 2010; Ershova et al. 2015). Bottom salinity is one of the main environmental factors affecting demersal fish assemblages in the Chukchi Sea (Norcross et al. 2010) whereas surface salinity has been reported as an important factor influencing zooplankton distributions (Ershova et al. 2015). In our study, fish and zooplankton distribution patterns were associated with salinity. The occurrence of these associations coincided with sea ice formation and melt as well as with autumn strengthening of local winds at the CEO.

Seasonal and annual variability

There was no single scale of seasonal variability in fish and zooplankton metrics values, nor could seasonal time scales be attributed to a single environmental factor. Scales of seasonal variability and scale-dependent associations with environmental factors were also different for fish and zooplankton.

A seasonality of 3 months in zooplankton metrics corresponded to temporal patterns in sea ice concentration, whereas 3-month cycles in fish metrics appeared related to variability in water salinity. Temporal patterns in sea ice formation and melt modulate light irradiance and stratification of the water column, directly affecting temporal patterns of ice algae, phytoplankton (Palmer et al. 2014), and in turn, zooplankton production (Matsuno et al. 2011; Questel et al. 2013; Amano et al. 2019). Primary production by ice

algae underneath the ice is initiated during late winter–early spring (typically in March) at very low light intensities and constitute an early food source for zooplankton (Søreide et al. 2010). In spring, increased insolation, stratification from ice melt, and availability of nutrients accumulated during the winter, trigger the onset of a phytoplankton bloom that sustains annual zooplankton production (Søreide et al. 2010; Leu et al. 2011, 2015; Arrigo et al. 2012). In particular, *C. glacialis* has synchronized its seasonal vertical migrations, reproduction, and growth to these two bloom events. The ice algae bloom is thought to fuel early maturation and reproduction of zooplankton whereas the subsequent phytoplankton bloom provides high-quality food to the resulting zooplankton offspring (Søreide et al. 2010; Leu et al. 2011; Barber et al. 2015). This tight control exerted by seasonal sea ice on densities and vertical distributions of zooplankton is consistent with patterns observed in our study.

Temperature is known to structure habitats of Arctic fish species and to affect their distribution (Benoit et al. 2014; Sigler et al. 2017), growth (Bouchard and Fortier 2011; Laurel et al. 2016), and abundance (Mueter et al. 2016). Chukchi shelf water masses that start cooling approximately in October and remain close to the freezing point through April warm in summer when northward transport of warmer waters from the Bering Sea is highest (Danielson et al. 2017a; Lu et al. 2020). In the NE Chukchi Sea, the arrival of warmer waters from the Bering Sea generally increases the abundance of organisms in summer through the addition of imported boreal organisms and enhancement of local growth (Questel et al. 2013; Ashjian et al. 2017). As water temperature cools in autumn, densities of organisms decrease. This has been attributed to unsuccessful overwintering of boreal species (Kitamura et al. 2017) or horizontal migrations of local species to overwinter in adjacent deeper waters (Kosobokova 1999; Benoit et al. 2008, 2010; Geoffroy et al. 2011). We observed water temperature-associated variability in fish metrics at the ~5-month period mainly from late spring to early fall, which corresponds to transitional periods from cold to warm and return to cold “seasons”. Similar patterns in fish location and dispersion at the ~5-month scale might also be indicative of seasonal vertical migrations associated with species life cycles (i.e. ontogenetic migrations, Geoffroy et al. 2016; LeBlanc et al. 2019) and behavioral changes (e.g. summer shoaling, Gjelland et al. 2009; Benoit et al. 2010) that typically occur from late spring to fall. However, variability in the vertical distributions of zooplankton species during these transitional periods seemed to respond to seasonal transitions from ice covered to open waters (and the reverse), and changes in wind speed. These two factors affect stratification of the water column, that in turn, modulate the timing and amplitude of primary production blooms. Some zooplankton species (e.g. *C. glacialis*) perform ontogenetic seasonal vertical

migrations that are tightly synchronized with blooms events (Søreide et al. 2010; Darnis and Fortier 2014).

Similarly, ~4-month cycles in zooplankton densities associated with air temperature and light irradiance at the CEO might be indicative of transitional periods between seasons. During these periods high variations in zooplankton densities are expected in response to changes in sun radiation and air temperature that control the onset of primary production (Søreide et al. 2010). Shorter seasonal cycles in zooplankton, compared to fish, could be associated with a faster response to changes in the environment and synchronicity of their life cycles to temporal patterns in food availability that are triggered mainly by changes in irradiance (Mundy et al. 2014). Longer seasonal cycles in fish are possibly explained by slower changes in water temperature throughout the year.

Variations in water temperature, sea ice concentration, light irradiance, and wind throughout a year shape the conspicuous annual cycles in fish and zooplankton metrics at the CEO. As described above, these factors play a key role in pelagic organisms' growth, reproduction, and distribution. Temperature regulates the growth rate of fish and zooplankton, while light irradiance, sea ice concentration and winds modulate primary and secondary production, either directly or through the modulation of light and nutrient availability. Biological interactions might also play a role shaping fish and zooplankton temporal patterns in addition to the physical environment. In particular, predation pressure could be responsible for the 9-month cycles observed in zooplankton patchiness instead of the annual cycle observed for all other metrics. Formation of dense patches of zooplankton individuals have been described as a strategy to reduce predation risk (Majaneva et al. 2013).

Importance and applications

The need to address scale dependency of biological patterns is well recognized in ecological literature (Stommel 1963; Haury et al. 1978; Levin 1992; Schneider 1994). Understanding temporal variability across a broad range of scales is essential to derive general conclusions about species abundance and behavior dynamics. As demonstrated in this study, fish and zooplankton metrics not only undergo variability over a range of temporal scales but also the relative importance of these scales may vary through time. As a result, an extrapolation of observed patterns from a short temporal extent may not be representative of patterns occurring at other times of the year. This emphasizes the importance of continuous year-round studies to obtain a complete description of biological patterns in high latitude marine ecosystems. Scale- and time-dependent characterization of marine ecosystems requires continuous, high-resolution, long-term datasets that are not possible to obtain using traditional vessel-based sampling methods, especially in high latitudes.

The use of active acoustics integrated with other sensors in ocean observing platforms provides simultaneous measurements of multiple ecosystem components at high temporal resolution over long periods. Time–frequency decomposition of biological and physical series using wavelets and wavelet coherence enabled identification of dominant scales of variability, located the occurrence of those periodicities in time, and helped identify potential environmental processes associated with observed biological patterns. Studies of temporal variability typically look at variations in the amplitude of a variable in the time domain (e.g. Gaston and McArdle 1994). Even though variability is rarely used as a response variable to assess the influence of environmental disturbances, it is an extremely sensitive metric that can provide ecological information about underlying causal processes (Fraterrigo and Rusak 2008).

A characterization of scale-dependent biological patterns and associations with environmental factors is a first step towards a mechanistic understanding of ecosystem dynamics. This understanding is necessary to predict biological responses to environmental change. Rapid changes in the Chukchi physical environment have been reported and further changes are expected (Wood et al. 2015; Woodgate 2018). Some of these changes include reduced seasonal sea ice extent and duration, increased ocean temperatures, and increased freshwater content (Stroeve et al. 2007; Polyakov et al. 2010; Steele et al. 2010; Lu et al. 2020). Changes in the physical environment are expected to alter amplitude, periodicity, and the timing of biological production (Grebmeier 2012). Predicting the potential direction and magnitude of these changes will help design or improve mitigation strategies and management of Arctic marine species. Polar cod has been identified as a species of potential commercial importance in the Arctic Fishery Management Plan (NPFMC 2009). In the context of potential harvest, a characterization of scales of variability in polar cod abundance can be used to inform stock assessments that provide accurate biomass estimates and detect trends in population variability. A characterization of scale-dependent temporal patterns can also be used to inform the design of monitoring programs to ensure the detection of change in an already highly variable environment. Both sampling resolution and extent can be defined using natural scales of biological variation rather than arbitrary or convenience scales (e.g. annual surveys during open water season), enabling the deconvolution of “natural” variability from differences in the timing or resolution of sampling. A continuous, long term characterization of biological patterns can be used to identify a baseline, and subsequent deviations can be quantified to characterize and determine change.

How generic temporal patterns observed at the CEO are of patterns occurring elsewhere in the Arctic is uncertain. A quantification of the spatial scope of our point measurements

at the CEO is underway and will provide a better understanding of the area represented by our temporally-indexed measurements. Also, direct comparisons among high latitude ecosystems will be possible as time series with similar temporal scopes become available from other parts of the Arctic and Antarctic.

Supplementary Information The online version contains supplementary material available at <https://doi.org/10.1007/s00300-021-02844-1>.

Acknowledgements The authors would like to acknowledge NPRB for a Graduate Student Research Award, the Oil Spill Research Institute for a Graduate Research Fellowship and Fulbright-ANII for a graduate student fellowship program. We thank Caroline Bouchard and two anonymous reviewers for comments and suggestions that improved this manuscript. We thank the captains and crews of the M/V Norseman II, R/V Sikuliaq, R/V Ocean Starr, and USCGC Healy for CEO mooring turnarounds, along with chief scientists C. Ashjian, R. Hopcroft, K. Iken, R. McCabe, and P. Winsor. SLD acknowledges CEO support from AOOS grants G9046 and G11133 and NPRB projects #1426 and L36-00A (NPRB publication # 1901).

Author contributions SG and JKH conceived and designed this study, with input from SLD. SLD provided the Chukchi Ecosystem Observatory datasets. SG processed and analyzed the data, advised by JKH and SLD. SG wrote the manuscript, JKH and SLD revised the manuscript.

Funding S.G received support from North Pacific Research Board Graduate Student Research Award, and Oil Spill Research Institute Graduate Research Fellowship. The Chukchi Ecosystem Observatory receives operations and equipment funding from the North Pacific Research Board via project #1426 and #19 and the Alaska Ocean Observing System via award #NA11NOS0120020.

Declarations

Conflict of interest The authors declare that they have no conflict of interest.

Informed consent All authors consent to the publication of this manuscript.

References

- Amano K, Abe Y, Matsuno K, Yamaguchi A (2019) Yearly comparison of the planktonic chaetognath community in the Chukchi Sea in the summers of 1991 and 2007. *Polar Sci* 19:112–119. <https://doi.org/10.1016/j.polar.2018.11.011>
- Arrigo KR, Perovich DK, Pickart RS et al (2014) Phytoplankton blooms beneath the sea ice in the Chukchi sea. *Deep-Sea Res II* 105:1–16. <https://doi.org/10.1016/j.dsr2.2014.03.018>
- Arrigo KR, Perovich DK, Pickart RS et al (2012) Massive phytoplankton blooms under arctic sea ice. *Science*. <https://doi.org/10.1126/science.1215065>
- Ashjian CJ, Campbell RG, Gelfman C et al (2017) Mesozooplankton abundance and distribution in association with hydrography on Hanna Shoal, NE Chukchi Sea, during August 2012 and 2013. *Deep-Sea Res II* 144:21–36. <https://doi.org/10.1016/j.dsr2.2017.08.012>
- Ashjian CJ, Campbell RG, Welch HE et al (2003) Annual cycle in abundance, distribution, and size in relation to hydrography of important copepod species in the western Arctic Ocean. *Deep Res I* 50:1235–1261. [https://doi.org/10.1016/S0967-0637\(03\)00129-8](https://doi.org/10.1016/S0967-0637(03)00129-8)
- Barber DG, Hop H, Mundy CJ et al (2015) Selected physical, biological and biogeochemical implications of a rapidly changing Arctic Marginal Ice Zone. *Prog Oceanogr* 139:122–150. <https://doi.org/10.1016/j.pocean.2015.09.003>
- Barber WE, Smith RL, Vallarino M, Meyer RM (1997) Demersal fish assemblages of the northeastern Chukchi Sea, Alaska. *Fish Bull* 95:195–209
- Benoit D, Simard Y, Fortier L (2014) Pre-winter distribution and habitat characteristics of polar cod (*Boreogadus saida*) in south-eastern Beaufort Sea. *Polar Biol* 37:149–163. <https://doi.org/10.1007/s00300-013-1419-0>
- Benoit D, Simard Y, Fortier L (2008) Hydroacoustic detection of large winter aggregations of Arctic cod (*Boreogadus saida*) at depth in ice-covered Franklin Bay (Beaufort Sea). *J Geophys Res Ocean* 113:1–9. <https://doi.org/10.1029/2007JC004276>
- Benoit D, Simard Y, Gagné J et al (2010) From polar night to midnight sun: Photoperiod, seal predation, and the diel vertical migrations of polar cod (*Boreogadus saida*) under landfast ice in the Arctic Ocean. *Polar Biol* 33:1505–1520. <https://doi.org/10.1007/s00300-010-0840-x>
- Berge J, Cottier F, Last KS et al (2009) Diel vertical migration of Arctic zooplankton during the polar night. *Biol Lett* 5:69–72. <https://doi.org/10.1098/rsbl.2008.0484>
- Berge J, Renaud PE, Darnis G et al (2015) In the dark: a review of ecosystem processes during the Arctic polar night. *Prog Oceanogr* 139:258–271. <https://doi.org/10.1016/j.pocean.2015.08.005>
- Bivand R, Lewin-Koh N (2020) maptools: Tools for handling spatial objects. R package version 1.0-2. <https://CRAN.R-project.org/package=maptools>
- Blachowiak-Samolyk K, Kwasniewski S, Richardson K et al (2006) Arctic zooplankton do not perform diel vertical migration (DVM) during periods of midnight sun. *Mar Ecol Prog Ser* 308:101–116. <https://doi.org/10.3354/meps308101>
- Bluhm BA, Iken K, Hopcroft RR (2010) Observations and exploration of the Arctic's Canada Basin and the Chukchi Sea: The Hidden Ocean and RUSALCA expeditions. *Deep-Sea Res II* 57:1–4. <https://doi.org/10.1016/j.dsr2.2009.08.001>
- Born EW, Teilmann J, Acquarone M, Riget FF (2004) Habitat Use of Ringed Seals (*Phoca hispida*) in the North Water Area (North Baffin Bay). *Arctic* 57:129–142
- Bouchard C, Fortier L (2011) Circum-arctic comparison of the hatching season of polar cod *Boreogadus saida*: a test of the freshwater winter refuge hypothesis. *Prog Oceanogr* 90:105–116. <https://doi.org/10.1016/j.pocean.2011.02.008>
- Burgos JM, Horne JK (2008) Characterization and classification of acoustically detected fish spatial distributions. *ICES J Mar Sci* 65:1235–1247. <https://doi.org/10.1093/icesjms/fsn087>
- Campbell HA, Fraser KPP, Bishop CM et al (2008) Hibernation in an Antarctic fish: on ice for winter. *PLoS ONE* 3:e1743. <https://doi.org/10.1371/journal.pone.0001743>
- Cazelles B, Chavez M, Berteaux D et al (2008) Wavelet analysis of ecological time series. *Oecologia* 156:287–304. <https://doi.org/10.1007/s00442-008-0993-2>
- Cohen JH, Berge J, Moline MA et al (2015) Is ambient light during the high Arctic polar night sufficient to act as a visual cue for zooplankton? *PLoS ONE* 10:1–12. <https://doi.org/10.1371/journal.pone.0126247>
- Cohen JH, Forward RBJ (2009) Zooplankton diel vertical migration: a review of proximate control. *Oceanogr Mar Biol Annu Rev* 47:77–110

- Cottier FR, Tarling GA, Wold A, Falk-Petersen S (2006) Unsynchronized and synchronized vertical migration of zooplankton in a high arctic fjord. *Limnol Oceanogr* 51:2586–2599. <https://doi.org/10.4319/lo.2006.51.6.2586>
- Daase M, Falk-Petersen HHS (2016) Small-scale diel vertical migration of zooplankton in the High Arctic. *Polar Biol* 39:1213–1223. <https://doi.org/10.1007/s00300-015-1840-7>
- Dale T, Kaartvedt S (2000) Diel patterns in stage-specific vertical migration of *Calanus finmarchicus* in habitats with midnight sun. *ICES J Mar Sci* 57:1800–1818. <https://doi.org/10.1006/jmsc.2000.0961>
- Danielson SL, Eisner L, Ladd C et al (2017a) A comparison between late summer 2012 and 2013 water masses, macronutrients, and phytoplankton standing crops in the northern Bering and Chukchi Seas. *Deep-Sea Res II* 135:7–26. <https://doi.org/10.1016/j.dsr2.2016.05.024>
- Danielson SL, Iken K, Hauri C, et al (2017b) Collaborative approaches to multi-disciplinary monitoring of the Chukchi shelf marine ecosystem: Networks of networks for maintaining long-term Arctic observations. In: MTS/IEEE Oceans17 conference proceedings, Anchorage, AK, USA, 18–21 September 2017, pp 1–7
- Darnis G, Fortier L (2014) Temperature, food and the seasonal vertical migration of key arctic copepods in the thermally stratified Amundsen Gulf (Beaufort Sea, Arctic Ocean). *J Plankton Res* 36:1092–1108. <https://doi.org/10.1093/plankt/fbu035>
- Darnis G, Hobbs L, Geoffroy M et al (2017) From polar night to midnight sun: Diel vertical migration, metabolism and biogeochemical role of zooplankton in a high Arctic fjord (Kongsfjorden, Svalbard). *Limnol Oceanogr* 62:1586–1605. <https://doi.org/10.1002/lno.10519>
- De Robertis A, McKelvey DR, Ressler PH (2010) Development and application of an empirical multifrequency method for backscatter classification. *Can J Fish Aquat Sci* 67:1459–1474. <https://doi.org/10.1139/F10-075>
- De Robertis A, Taylor K, Wilson CD, Farley EV (2017) Abundance and distribution of Arctic cod (*Boreogadus saida*) and other pelagic fishes over the U.S. Continental Shelf of the Northern Bering and Chukchi Seas. *Deep-Sea Res II* 135:51–65. <https://doi.org/10.1016/j.dsr2.2016.03.002>
- Elliott SM, Ashjian CJ, Feng Z et al (2017) Physical control of the distributions of a key Arctic copepod in the Northeast Chukchi Sea. *Deep-Sea Res II* 144:37–51. <https://doi.org/10.1016/j.dsr2.2016.10.001>
- Ershova EA, Hopcroft RR, Kosobokova KN et al (2015) Long-term changes in Summer zooplankton communities of the Western Chukchi Sea, 1945–2012. *Oceanography* 28:100–115. <https://doi.org/10.5670/oceanog.2015.60>
- Falk-Petersen S, Leu E, Berge J et al (2008) Vertical migration in high Arctic waters during autumn 2004. *Deep-Sea Res II* 55:2275–2284. <https://doi.org/10.1016/j.dsr2.2008.05.010>
- Falk-Petersen S, Mayzaud P, Kattner G, Sargent JR (2009) Lipids and life strategy of Arctic *Calanus*. *Mar Biol Res* 5:18–39. <https://doi.org/10.1080/17451000802512267>
- Fortier M, Fortier L, Hattori H et al (2001) Visual predators and the diel vertical migration of copepods under Arctic sea ice during the midnight sun. *J Plankton Res* 23:1263–1278
- Fraterrigo JM, Rusak JA (2008) Disturbance-driven changes in the variability of ecological patterns and processes. *Ecol Lett* 11:756–770. <https://doi.org/10.1111/j.1461-0248.2008.01191.x>
- Fujiwara A, Nishino S, Matsuno K et al (2018) Changes in phytoplankton community structure during wind-induced fall bloom on the central Chukchi shelf. *Polar Biol* 41:1279–1295. <https://doi.org/10.1007/s00300-018-2284-7>
- Gaston KJ, McArdle BH (1994) The temporal variability of animal abundances: measures, methods and patterns. *Philos Trans R Soc London* 345:335–358
- Geoffroy M, Cottier FR, Berge J, Inall ME (2017) AUV-based acoustic observations of the distribution and patchiness of pelagic scattering layers during midnight sun. *ICES J Mar Sci* 74:2342–2353. <https://doi.org/10.1093/icesjms/fsw158>
- Geoffroy M, Majewski A, LeBlanc M et al (2016) Vertical segregation of age-0 and age-1+ polar cod (*Boreogadus saida*) over the annual cycle in the Canadian Beaufort Sea. *Polar Biol* 39:1023–1037. <https://doi.org/10.1007/s00300-015-1811-z>
- Geoffroy M, Robert D, Darnis G, Fortier L (2011) The aggregation of polar cod (*Boreogadus saida*) in the deep Atlantic layer of ice-covered Amundsen Gulf (Beaufort Sea) in winter. *Polar Biol* 34:1959–1971. <https://doi.org/10.1007/s00300-011-1019-9>
- Gjelland KØ, Bøhn T, Horne JK et al (2009) Planktivore vertical migration and shoaling under a subarctic light regime. *Can J Fish Aquat Sci* 66:525–539. <https://doi.org/10.1139/F09-014>
- Goddard P, Lauth R, Armistead C (2014) Results of the 2012 Chukchi Sea bottom trawl survey of bottomfishes, crabs, and other demersal macrofauna. U.S. Dep. Commer., NOAA Tech, Memo, NMFS-AFSC-278, Seattle
- Godø OR, Handegard NO, Browman HI et al (2014) Marine ecosystem acoustics (MEA): quantifying processes in the sea at the spatio-temporal scales on which they occur. *ICES J Mar Sci* 71:2357–2369. <https://doi.org/10.1093/icesjms/fsu116>
- Gonzalez S, Horne JK, Ward EJ (2019) Temporal variability in pelagic biomass distributions at wave and tidal sites and implications for standardization of biological monitoring. *Int Mar Energy J* 2:15–28
- Gradinger R (2009) Sea-ice algae: Major contributors to primary production and algal biomass in the Chukchi and Beaufort Seas during May/June 2002. *Deep-Sea Res II* 56:1201–1212. <https://doi.org/10.1016/j.dsr2.2008.10.016>
- Grebmeier JM (2012) Shifting patterns of life in the Pacific Arctic and sub-Arctic seas. *Ann Rev Mar Sci* 4:63–78. <https://doi.org/10.1146/annurev-marine-120710-100926>
- Grebmeier JM, Bluhm BA, Cooper LW et al (2015) Ecosystem characteristics and processes facilitating persistent macrobenthic biomass hotspots and associated benthivory in the Pacific Arctic. *Prog Oceanogr* 136:92–114. <https://doi.org/10.1016/j.pocean.2015.05.006>
- Grebmeier JM, Cooper LW, Feder HM, Sirenko BI (2006) Ecosystem dynamics of the Pacific-influenced Northern Bering and Chukchi Seas in the Amerasian Arctic. *Prog Oceanogr* 71:331–361. <https://doi.org/10.1016/j.pocean.2006.10.001>
- Hannay DE, Delarue J, Mouy X et al (2013) Marine mammal acoustic detections in the northeastern Chukchi Sea, September 2007–July 2011. *Cont Shelf Res* 67:127–146. <https://doi.org/10.1016/j.csr.2013.07.009>
- Hauri C, Danielson S, McDonnell AMP et al (2018) From sea ice to seals: a moored marine ecosystem observatory in the Arctic. *Ocean Sci Discuss* 14:1423–1433. <https://doi.org/10.5194/os-2018-82>
- Hauri LR, McGowan JA, Wiebe PH (1978) Patterns and processes in the time-space scales of plankton distributions. In: Steele JH (ed) Spatial pattern in plankton communities NATO conference series (IV marine sciences), vol 3. Springer, Boston
- Hays GC (2003) A review of the adaptive significance and ecosystem consequences of zooplankton diel vertical migrations. *Hydrobiologia* 503:163–170. <https://doi.org/10.1023/B:HYDR.0000008476.23617.b0>
- Hersbach H, Bell B, Berrisford P, Biavati G, Horányi A, Muñoz Sabater J, Nicolas J, Peubey C, Radu R, Rozum I, Schepers D, Simmons A, Soci C, Dee D, Thépaut J-N (2018) ERA5 hourly data on single levels from 1979 to present. Copernicus Climate Change Service (C3S) Climate Data Store (CDS). <https://doi.org/10.24381/cds.adbb2d47>. Accessed 1 Mar 2020

- Hewitt JE, Thrush SF, Dayton PK, Bonsdorff E (2007) The effect of spatial and temporal heterogeneity on the design and analysis of empirical studies of scale-dependent systems. *Am Nat* 169:398–408. <https://doi.org/10.1086/510925>
- Hill V, Ardyna M, Lee SH, Varela DE (2018) Decadal trends in phytoplankton production in the Pacific Arctic Region from 1950 to 2012. *Deep-Sea Res II* 152:82–94. <https://doi.org/10.1016/j.dsr2.2016.12.015>
- Hobbs L, Cottier F, Last K, Berge J (2018) Pan-Arctic diel vertical migration during the polar night. *Mar Ecol Prog Ser* 605:61–72. <https://doi.org/10.3354/meps12753>
- Hopcroft RR, Day RH (2013) Introduction to the special issue on the ecology of the northeastern Chukchi Sea. *Cont Shelf Res* 67:1–4. <https://doi.org/10.1016/j.csr.2013.06.017>
- Hopcroft RR, Kosobokova KN, Pinchuk AI (2010) Zooplankton community patterns in the Chukchi Sea during summer 2004. *Deep-Sea Res II* 57:27–39. <https://doi.org/10.1016/j.dsr2.2009.08.003>
- Horne JK, Schneider DC (1994) Analysis of scale-dependent processes with dimensionless ratios. *Oikos* 70:201–211. <https://doi.org/10.2307/3545631>
- Jay CV, Fischbach AS, Kochnev AA (2012) Walrus areas of use in the Chukchi Sea during sparse sea ice cover. *Mar Ecol Prog Ser* 468:1–13. <https://doi.org/10.3354/meps10057>
- Kang M, Furusawa M, Miyashita K (2002) Effective and accurate use of difference in mean volume backscattering strength to identify fish and plankton. *ICES J Mar Sci* 59:794–804. <https://doi.org/10.1006/jmsc.2002.1229>
- Kelley D, Richards C (2021) oce: Analysis of oceanographic data. R package version 1.3-0. <https://CRAN.R-project.org/package=oce>
- Kitamura M, Amakasu K, Kikuchi T, Nishino S (2017) Seasonal dynamics of zooplankton in the southern Chukchi Sea revealed from acoustic backscattering strength. *Cont Shelf Res* 133:47–58. <https://doi.org/10.1016/j.csr.2016.12.009>
- Korneliusen RJ, Ona E (2003) Synthetic echograms generated from the relative frequency response. *ICES J Mar Sci* 60:636–640. [https://doi.org/10.1016/S1054-3139\(03\)00035-3](https://doi.org/10.1016/S1054-3139(03)00035-3)
- Kosobokova KN (1999) The reproductive cycle and life history of the Arctic copepod *Calanus glacialis* in the White Sea. *Polar Biol* 22:254–263
- Kuletz KJ, Ferguson MC, Hurley B et al (2015) Seasonal spatial patterns in seabird and marine mammal distribution in the eastern Chukchi and western Beaufort seas: identifying biologically important pelagic areas. *Prog Oceanogr* 136:175–200. <https://doi.org/10.1016/j.pocean.2015.05.012>
- Lalande C, Grebmeier JM, Hopcroft RR, Danielson SL (2020) Annual cycle of export fluxes of biogenic matter near Hanna Shoal in the northeast Chukchi Sea. *Deep-Sea Res II*. <https://doi.org/10.1016/j.dsr2.2020.104730>
- Lane PVZ, Llinás L, Smith SL, Pilz D (2008) Zooplankton distribution in the western Arctic during summer 2002: hydrographic habitats and implications for food chain dynamics. *J Mar Syst* 70:97–133. <https://doi.org/10.1016/j.jmarsys.2007.04.001>
- Last KS, Hobbs L, Berge J et al (2016) Moonlight drives ocean-scale mass vertical migration of zooplankton during the Arctic Winter. *Curr Biol* 26:244–251. <https://doi.org/10.1016/j.cub.2015.11.038>
- Laurel BJ, Spencer M, Iseri P, Copeman LA (2016) Temperature-dependent growth and behavior of juvenile Arctic cod (*Boreogadus saida*) and co-occurring North Pacific gadids. *Polar Biol* 39:1127–1135. <https://doi.org/10.1007/s00300-015-1761-5>
- LeBlanc M, Gauthier S, Garbus SE et al (2019) The co-distribution of Arctic cod and its seabird predators across the marginal ice zone in Baffin Bay. *Elementa* 7:1–18. <https://doi.org/10.1525/elementa.339>
- Leu E, Mundy CJ, Assmy P et al (2015) Arctic spring awakening: steering principles behind the phenology of vernal ice algal blooms. *Prog Oceanogr* 139:151–170. <https://doi.org/10.1016/j.pocean.2015.07.012>
- Leu E, Søreide JE, Hessen DO et al (2011) Consequences of changing sea-ice cover for primary and secondary producers in the European Arctic shelf seas: timing, quantity, and quality. *Prog Oceanogr* 90:18–32. <https://doi.org/10.1016/j.pocean.2011.02.004>
- Levin SA (1992) The problem of pattern and scale. *Ecology* 73:1943–1967
- Lin II (2012) Typhoon-induced phytoplankton blooms and primary productivity increase in the western North Pacific subtropical ocean. *J Geophys Res Ocean*. <https://doi.org/10.1029/2011JC007626>
- Logerwell E, Rand K, Danielson S, Sousa L (2018) Environmental drivers of benthic fish distribution in and around Barrow Canyon in the northeastern Chukchi Sea and western Beaufort Sea. *Deep-Sea Res II* 152:170–181. <https://doi.org/10.1016/j.dsr2.2017.04.012>
- Lorenzen CJ (1972) Extinction of light in the ocean by phytoplankton. *ICES J Mar Sci* 34:262–267. <https://doi.org/10.1093/icesjms/34.2.262>
- Lowry LF, Frost KJ (1981) Distribution, growth, and foods of Arctic cod (*Boreogadus saida*) in the Bering, Chukchi and Beaufort Seas. *Can Field-Naturalist* 95:186–191
- Lu K, Danielson S, Hedstrom K, Weingartner T (2020) Assessing the role of oceanic heat fluxes on ice ablation of the central Chukchi Sea Shelf. *Prog Oceanogr* 184:102313. <https://doi.org/10.1016/j.pocean.2020.102313>
- MacLennan D, Fernandes PG, Dalen J (2002) A consistent approach to definitions and symbols in fisheries acoustics. *ICES J Mar Sci* 59:365–369. <https://doi.org/10.1006/jmsc.2001.1158>
- Madureira LSP, Ward P, Atkinson A (1993) Differences in backscattering strength determined at 120 and 38 kHz for three species of Antarctic macroplankton. *Mar Ecol Prog Ser* 93:17–24. <https://doi.org/10.3354/meps093017>
- Majaneva S, Berge J, Renaud PE et al (2013) Aggregations of predators and prey affect predation impact of the Arctic ctenophore *Mertensia ovum*. *Mar Ecol Prog Ser* 476:87–100. <https://doi.org/10.3354/meps10143>
- Maslanik J, Stroeve J (1999) Near-real-time DMSP SSMIS daily polar gridded sea ice concentrations, version 1. NASA National Snow Ice and Data Center, Boulder
- Matley JK, Crawford RE, Dick TA (2012) Summer foraging behaviour of shallow-diving seabirds and distribution of their prey, Arctic cod (*Boreogadus saida*), in the Canadian Arctic. *Polar Res* 31:15894. <https://doi.org/10.3402/polar.v31i0.15894>
- Matsuno K, Yamaguchi A, Hirawake T, Imai I (2011) Year-to-year changes of the mesozooplankton community in the Chukchi Sea during summers of 1991, 1992 and 2007, 2008. *Polar Biol* 34:1349–1360. <https://doi.org/10.1007/s00300-011-0988-z>
- McIntire EJB, Fajardo A (2009) Beyond description: the active and effective way to infer processes from spatial patterns. *Ecology* 90:46–56. <https://doi.org/10.1890/07-2096.1>
- Moore SE, Stabeno PJ (2015) Synthesis of Arctic Research (SOAR) in marine ecosystems of the Pacific Arctic. *Prog Oceanogr* 136:1–11. <https://doi.org/10.1016/j.pocean.2015.05.017>
- Mueter FJ, Nahrgang J, John Nelson R, Berge J (2016) The ecology of gadid fishes in the circumpolar Arctic with a special emphasis on the polar cod (*Boreogadus saida*). *Polar Biol* 39:961–967. <https://doi.org/10.1007/s00300-016-1965-3>
- Mueter FJ, Weems J, Farley EV, Sigler MF (2017) Arctic Ecosystem Integrated Survey (Arctic Eis): Marine ecosystem dynamics in the rapidly changing Pacific Arctic Gateway. *Deep-Sea Res II* 135:1–6. <https://doi.org/10.1016/j.dsr2.2016.11.005>
- Mundy CJ, Gosselin M, Gratton Y et al (2014) Role of environmental factors on phytoplankton bloom initiation under landfast sea

- ice in Resolute Passage, Canada. *Mar Ecol Prog Ser* 497:39–49. <https://doi.org/10.3354/meps10587>
- Norcross BL, Holladay BA, Busby MS, Mier KL (2010) Demersal and larval fish assemblages in the Chukchi Sea. *Deep-Sea Res II* 57:57–70. <https://doi.org/10.1016/j.dsr2.2009.08.006>
- NPFMC (2009) Fishery management plan for fish resources of the arctic management area. NPFMC, Anchorage
- Palmer MA, Saenz BT, Arrigo KR (2014) Impacts of sea ice retreat, thinning, and melt-pond proliferation on the summer phytoplankton bloom in the Chukchi Sea, Arctic Ocean. *Deep-Sea Res II* 105:85–104. <https://doi.org/10.1016/j.dsr2.2014.03.016>
- Polyakov IV, Timokhov LA, Alexeev VA et al (2010) Arctic ocean warming contributes to reduced polar ice cap. *J Phys Oceanogr* 40:2743–2756. <https://doi.org/10.1175/2010JPO4339.1>
- Questel JM, Clarke C, Hopcroft RR (2013) Seasonal and interannual variation in the planktonic communities of the northeastern Chukchi Sea during the summer and early fall. *Cont Shelf Res* 67:23–41. <https://doi.org/10.1016/j.csr.2012.11.003>
- Randall JR, Busby MS, Spear AH, Mier KL (2019) Spatial and temporal variation of late summer ichthyoplankton assemblage structure in the eastern Chukchi Sea: 2010–2015. *Polar Biol* 42:1811–1824. <https://doi.org/10.1007/s00300-019-02555-8>
- Ressler PH, De RA, Warren JD et al (2012) Developing an acoustic survey of euphausiids to understand trophic interactions in the Bering Sea ecosystem. *Deep-Sea Res II* 65–70:184–195. <https://doi.org/10.1016/j.dsr2.2012.02.015>
- Roesch A, Schmidbauer H (2018) WaveletComp: Computational wavelet analysis. R package version 1.1. <https://CRAN.R-project.org/package=WaveletComp>
- Schneider DC (1994) Quantitative ecology: spatial and temporal scaling. Academic Press, San Diego
- Sigler MF, Mueter FJ, Bluhm BA et al (2017) Late summer zoogeography of the northern Bering and Chukchi seas. *Deep-Sea Res II* 135:168–189. <https://doi.org/10.1016/j.dsr2.2016.03.005>
- Søreide JE, Leu EVA, Berge J et al (2010) Timing of blooms, algal food quality and *Calanus glacialis* reproduction and growth in a changing Arctic. *Glob Chang Biol* 16:3154–3163. <https://doi.org/10.1111/j.1365-2486.2010.02175.x>
- Spear A, Duffy-Anderson J, Kimmel D et al (2019) Physical and biological drivers of zooplankton communities in the Chukchi Sea. *Polar Biol* 42:1107–1124. <https://doi.org/10.1007/s00300-019-02498-0>
- Steele M, Zhang J, Ermold W (2010) Mechanisms of summertime upper Arctic Ocean warming and the effect on sea ice melt. *J Geophys Res Ocean* 115:1–12. <https://doi.org/10.1029/2009JC005849>
- Stigebrandt A (1984) The North Pacific: a global-scale estuary. *J Phys Oceanogr* 14:464–470
- Stommel H (1963) Varieties of oceanographic experience: the ocean can be investigated as a hydrodynamical phenomenon as well as explored geographically. *Science* 139:572–576. <https://doi.org/10.1126/science.139.3555.572>
- Stroeve J, Holland MM, Meier W et al (2007) Arctic sea ice decline: faster than forecast. *Geophys Res Lett* 34:1–5. <https://doi.org/10.1029/2007GL029703>
- Torrence C, Compo GP (1998) A practical guide to wavelet analysis. *Bull Am Meteorol Soc* 79:61–78. [https://doi.org/10.1175/1520-0477\(1998\)079%3c0061:APGTWA%3e2.0.CO;2](https://doi.org/10.1175/1520-0477(1998)079%3c0061:APGTWA%3e2.0.CO;2)
- Urmy SS (2012) Temporal Variability and Bio-Physical Coupling in the Pelagic Fauna of Monterey Bay. Dissertation. University of Washington, Washington DC
- Urmy SS, Horne JK, Barbee DH (2012) Measuring the vertical distributional variability of pelagic fauna in Monterey Bay. *ICES J Mar Sci* 69:184–196. <https://doi.org/10.1093/icesjms/fst034>
- Viehman HA, Zydlewski GB (2017) Multi-scale temporal patterns in fish presence in a high-velocity tidal channel. *PLoS ONE* 12:1–20. <https://doi.org/10.1371/journal.pone.0176405>
- Wallace MI, Cottier FR, Berge J et al (2010) Comparison of zooplankton vertical migration in an ice-free and a seasonally ice-covered Arctic fjord: an insight into the influence of sea ice cover on zooplankton behavior. *Limnol Oceanogr* 55:831–845. <https://doi.org/10.4319/lo.2009.55.2.0831>
- Weingartner T, Aagaard K, Woodgate R, Danielson S (2005) Circulation on the north central Chukchi Sea shelf. *Deep-Sea Res II* 52:3150–3174. <https://doi.org/10.1016/j.dsr2.2005.10.015>
- Weingartner T, Dobbins E, Danielson S et al (2013) Hydrographic variability over the northeastern Chukchi Sea shelf in summer-fall 2008–2010. *Cont Shelf Res* 67:5–22. <https://doi.org/10.1016/j.csr.2013.03.012>
- Whitehouse GA, Aydin K, Essington TE, Hunt GL (2014) A trophic mass balance model of the eastern Chukchi Sea with comparisons to other high-latitude systems. *Polar Biol* 37:911–939. <https://doi.org/10.1007/s00300-014-1490-1>
- Wood KR, Bond NA, Danielson SL et al (2015) A decade of environmental change in the Pacific Arctic region. *Prog Oceanogr* 136:12–31. <https://doi.org/10.1016/j.pocean.2015.05.005>
- Woodgate RA (2018) Increases in the Pacific inflow to the Arctic from 1990 to 2015, and insights into seasonal trends and driving mechanisms from year-round Bering Strait mooring data. *Prog Oceanogr* 160:124–154. <https://doi.org/10.1016/j.pocean.2017.12.007>
- Zhao H, Shao J, Han G et al (2015) Influence of Typhoon Matsa on phytoplankton chlorophyll-A off East China. *PLoS ONE* 10:1–13. <https://doi.org/10.1371/journal.pone.0137863>

Publisher's Note Springer Nature remains neutral with regard to jurisdictional claims in published maps and institutional affiliations.